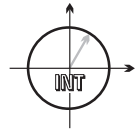




Universität Karlsruhe (TH)
Forschungsuniversität · gegründet 1825

Institut für Nachrichtentechnik
Prof. Dr.rer.nat. Friedrich K. Jondral



**Feasibility study of a
WCDMA direct air-to-ground link
in the UMTS licensed band**

Master's Thesis by

Dora Swamy Naidu Raghavarapu

Hauptreferent : Prof. Dr.rer.nat. Friedrich Jondral
Betreuer : Dipl.-Ing. Daniel Medina

Beginn : 25.01.06
Abgabe : 25.07.06

Acknowledgments

This master's thesis is presented in partial fulfillment of the requirements for the degree of Master of Science in the subject of “**Information and Communication Engineering**”. It has come to a successful completion not only with an individual effort, but also with the help of the following persons.

With a deep sense of gratitude, I wish to express my most sincere thanks to my supervisors, **Dipl.-Ing. Daniel Medina** and **Dipl.-Ing. Alexander Arkhipov**, for their immense help in planning and executing the work in time. The confidence and dynamism with which **Dr. Michael Schnell** guided the work requires no elaboration. On the other hand, profound knowledge and timely wit came as a boon under the guidance of **Prof. Dr. Friedrich Jondral**.

I would also like to thank **Dr. Armin Dammann** and the other colleagues of the Department of Communication Systems. Without their help, this thesis would have been incomplete.

The episode of acknowledgment would not be complete without mentioning my fellow research students at the Institute of Communications and Navigation in DLR.

I am grateful to my parents, who taught me the value of hard work by their own example. I would like to share this moment of happiness with my father, mother, brother and sister-in-law.

Finally, I would like to thank all those whose direct or indirect support helped me reach this milestone in time.

Munich, July 17, 2006

Contents

1	Introduction	1
1.1	Aim	1
1.2	Motivation	2
2	Overview of UMTS and WCDMA	7
2.1	Summary of the main parameters in WCDMA	7
2.2	Power Control	9
2.3	Softer and soft handovers	11
2.4	Radio Access Network Architecture	13
2.5	Services and Functions of the Physical Layer	16
2.5.1	Overview of L1 functions	17
3	Analysis of aircraft specific constraints	19
3.1	Propagation delay	21
3.2	Doppler shift	23
3.3	Handover	25
3.4	Interference	26
3.4.1	Forward link	26
3.4.2	Reverse Link	27
4	Air-to-ground link model	29
4.1	Concept description	29
4.2	Base station antenna study	32
5	Description of uplink WCDMA physical layer simulator	37
5.1	Overview of Spreading and Modulation	40
5.2	Channel	42
6	Simulation Results	45
6.1	Required UE power increase versus aircraft cell radius	49
7	Conclusions and Outlook	53
A	State of the art analysis	55
A.1	How voice will be added	55
A.2	Regulations	56

Contents

A.3	Some Players	56
A.3.1	Connexion by Boeing	56
A.3.2	OnAir	57
A.3.3	AirCell	57
A.3.4	Verizon AirFone	58
A.4	Auction News	59
B	Performance of RAKE Receiver	61
C	Mathematical derivations	63
	Bibliography	65

List of Figures

1.1	UMTS air interface architecture applied to aircraft	1
1.2	Vodafone's UMTS (red) and GSM (blue) coverage in Germany	3
1.3	Maximum physical channel bit rates in UMTS with HSDPA/HSUPA	5
2.1	Allocation of bandwidth in WCDMA in the time-frequency-code space	7
2.2	UMTS frequency allocation in Germany	8
2.3	Closed loop Power control in WCDMA	10
2.4	Softer Handover	11
2.5	Soft Handover	12
2.6	Inter-RNC soft handover	13
2.7	UMTS System Architecture	14
3.1	Illustration of airspace cell structure	19
3.2	Probability density function of flight path length within same cell	20
3.3	Worstcase scenario	21
3.4	Propagation delay definition according to 3GPP	22
3.5	PRACH propagation delay measurement report mapping	22
3.6	Transmit Power Control Timing	23
3.7	Evolution of Doppler shift as aircraft flies by over base station	24
3.8	Doppler shift	24
3.9	Excerpt from 3GPP I_{ur} interface specification	26
4.1	Geometry involved in the terrestrial and aircraft components	29
4.2	Typical directional pattern of a base station panel antenna for mobile communications	33
4.3	Interference estimation formula	34
4.4	Interference at base station receiver as aircraft flies by for three typical antennas (the graphs on the right are closeups)	35
5.1	Description of the Simulator	38
5.2	Overview of Spreading	41
6.1	Bit and block error rate curves for user data rate of 384 Kbps, AWGN channel	45
6.2	Bit and block error rate curves for user data rate of 12.2 Kbps, AWGN channel	47
6.3	Bit and block error rate curves for user data rate of 384 Kbps, MP channel, TPC OFF	47

List of Figures

6.4	Bit and block error curves rate for user data rate of 384 Kbps, MP channel, TPC ON	48
6.5	Dependency of the airspace cell size with the cost in terms of mobile terminal power increase for AWGN channel with 0° antenna downtilt	50
6.6	Dependency of the airspace cell size with the cost in terms of mobile terminal power increase for AWGN channel with 16° antenna downtilt	50
6.7	Dependency of the airspace cell size with the cost in terms of mobile terminal power increase for AWGN and MP channel (TPC) with 0° antenna downtilt . . .	51
B.1	Uncoded bit error rate check	62
C.1	Computation of $f_R(r)$	63

Abbreviations

Acronym	Description
3GPP	3rd Generation Partnership Project
AWGN	Additive White Gaussian Noise
BER	Bit Error Rate
BLER	Block Error Rate
BoD	Bandwidth on Demand
BPSK	Binary Phase Shift Keying
BS	Base Station
CDMA	Code Division Multiple Access
DL	Downlink
DCH	Dedicated Channel
DCCH	Dedicated Control Channel
DPCCH	Dedicated Physical Control Channel
DPDCH	Dedicated Physical Data Channel
DS-CDMA	Direct Spread Code Division Multiple Access
DSCH	Downlink Shared Channel
DTCH	Dedicated Traffic Channel
E-DCH	Enhanced Uplink DCH
EDGE	Enhanced Data Rates for GSM Evolution
EIRP	Effective Isotropic Radiated Power
FCC	Federal Communication Commission
FDD	Frequency Division Duplex
FDMA	Frequency Division Multiple Access
GGSN	Gateway GPRS Source Node
GPRS	General Packet Radio System
GPS	Global Positioning System
GSM	Global System for Mobile Communications
HSDPA	High Speed Downlink Packet Access
HS-DSCH	High Speed Downlink Shared Channel
HSUPA	High Speed Uplink Packet Access
IP	Internet Protocol
LAN	Local Area Network
MAC	Medium Access Control
ME	Mobile Equipment
MRC	Maximum Ratio Combining

Abbreviations

Acronym	Description
MS	Mobile Station
MSC	Mobile Services Switching Centre
PC	Power Control
PCCC	Parallel Concatenated Convolutional Coder
PLMN	Public Land Mobile Network
PRACH	Physical Random Access Channel
PS	Packet Switched
PSCH	Physical Shared Channel
PSTN	Public Switched Telephone Network
QAM	Quadrature Amplitude Modulation
QoS	Quality of Service
QPSK	Quadrature Phase Shift Keying
RAN	Radio Access Network
RNC	Radio Network Controller
SF	Spreading Factor
SGSN	Serving GPRS Support Node
SIR	Signal to Interference Ratio
SNR	Signal to Noise Ratio
TDMA	Time Division Multiple Access
TPC	Transmission Power Control
TTI	Transmission Time Interval
UE	User Equipment
UL	Uplink
UMTS	Universal Mobile Telecommunication Services
UTRA	UMTS Terrestrial Radio Access
UTRAN	UMTS Terrestrial Radio Access Network
WCDMA	Wideband CDMA, Code Division Multiple Access
WLAN	Wireless Local Area Network

Abbreviations

1 Introduction

1.1 Aim

The aim of this master's thesis is to assess the suitability of UMTS for aeronautical communications. Specifically, we wish to determine how existing UMTS networks may be accessed by aircraft with a direct air-to-ground communication link to provide onboard connectivity (e.g. Internet access).

This thesis studies the feasibility of using the UTRA FDD air interface, also denoted as U_u interface in the 3GPP specifications. Throughout this work, the UE (User Equipment) is assumed to be an aircraft equipped with a WCDMA transceiver. Every aircraft has at least one radio link to a UTRAN access point (Node B) on the ground. Our model is shown in Figure 1.1.

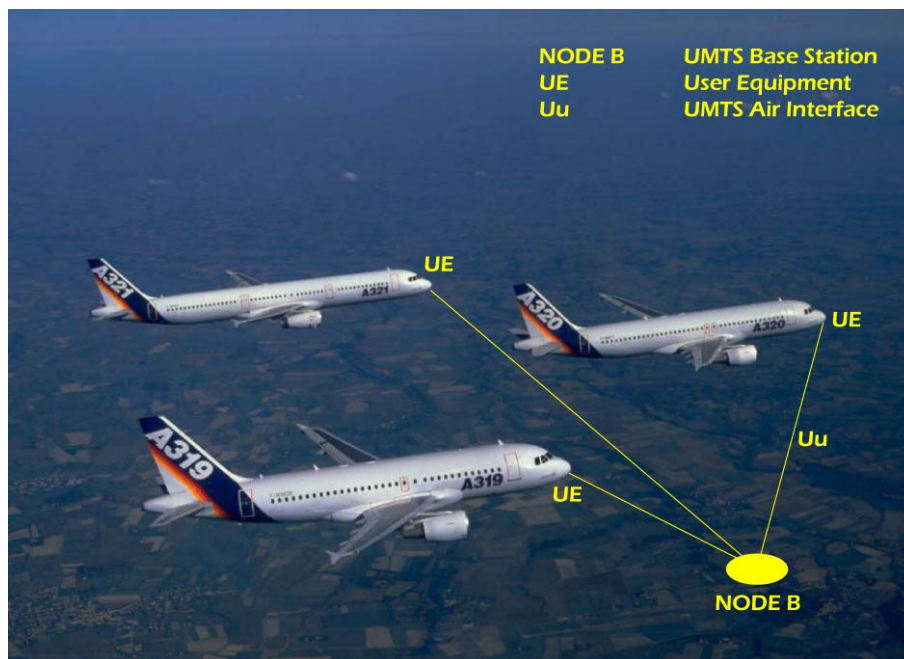


Figure 1.1: UMTS air interface architecture applied to aircraft

First, the suitability of UMTS to accommodate an air-to-ground component has been investigated in terms of the required changes in the ground infrastructure, cell sizes, link budget and interference emerging from the fact that an airborne UMTS user is transmitting. It is expected that the

1 Introduction

ground infrastructure has to be adapted to the aeronautical extension by applying separate antennas pointing toward the sky and, thus, extending UMTS into the third dimension. Reasonable cell sizes for this extension have been defined, taking into account the mobility characteristics of aircraft.

Second, a physical layer simulator for uplink UTRA FDD has been implemented in JAVA. The transmitter of this simulator comprises the UMTS specific channel coding, interleaving and spreading, whereas the receiver consists of the respective despreader, deinterleaver and decoder. Simulations have been performed to determine the necessary transmit power increase at a terrestrial transmitter which is required to maintain link performance in presence of aircraft generated interference. Using these results, the interference assessment has been identified.

1.2 Motivation

Today, aircraft seem to be the last remaining islands left for mobile communications and Internet access to reach. Research is going on to determine how multimedia communication services can be provided to passengers on board in a cost-efficient fashion. Inflight internet has become a reality only very recently, with the emergence of the first satellite-based systems, such as "Connexion by Boeing". These systems, however, rely on expensive infrastructure (satellites), and therefore result inevitably in a high price for the end user.

UMTS, one of the most important third generation terrestrial mobile communication systems, is now available in many parts of Europe and the rest of the world. This, together with the fact that many short range aircraft fly mainly over landmasses, where one or more public land mobile networks are in operation on the ground, motivates this investigation to find out how, if possible, aircraft could be interfaced into the ground infrastructure as if they were flying mobile nodes, reusing as much as possible existing technology (both hardware and software).

UMTS networks are currently being deployed all over Europe, where the main cities have already enjoyed 3G coverage for some time. Figure 1.2 shows Vodafone's GSM and UMTS coverage in Germany in early 2006. Other UMTS network operators in Germany (T-Mobile, O₂ and E-plus) have similar coverage maps. GSM is available almost every where, whereas UMTS coverage is still limited to large and medium-sized cities, exhibiting a discontinuous distribution. However, it seems reasonable to expect UMTS to be available almost everywhere in a few years, just as GSM today.

WCDMA (Wideband Code Division Multiple Access) is the main third generation air interface, and its deployment has been started in Europe and Asia, including Japan and Korea, in the same frequency band around 2 GHz. The large market for WCDMA and its flexible multimedia capabilities will create new business opportunities for manufacturers, operators and the providers of content and applications. It is for this reason that we have chosen to focus on WCDMA as a candidate for radio access technology to provide low cost onboard connectivity on short range

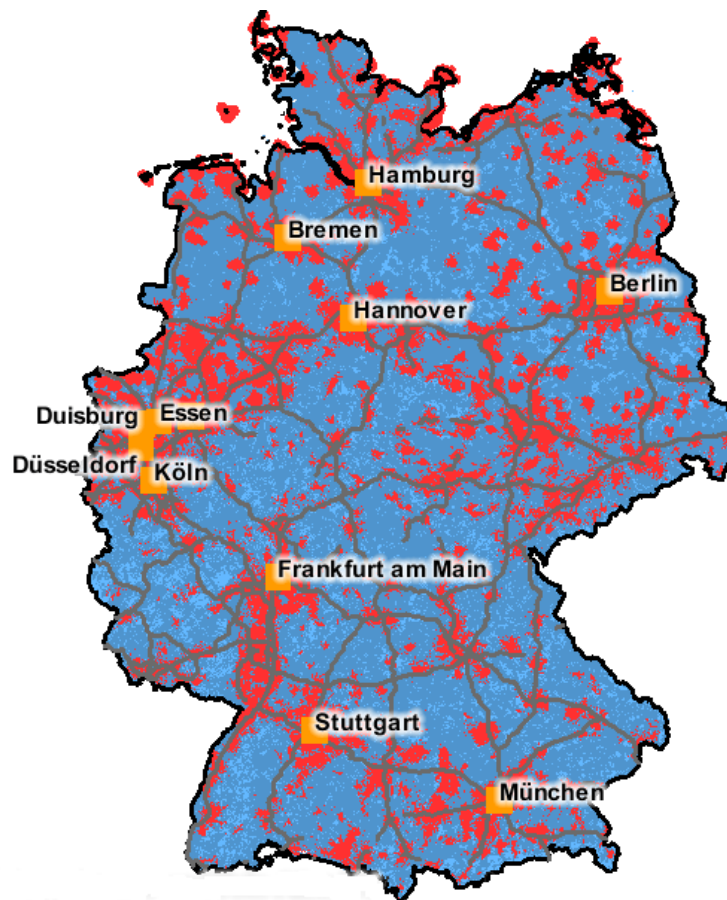


Figure 1.2: Vodafone's UMTS (red) and GSM (blue) coverage in Germany

flights with a direct air-to-ground communication link.

Another reason for choosing UMTS as a candidate for a direct air-to-ground link can be seen by considering the data rates that this technology can offer. In general, an aircraft will have a fairly high demand in terms of data rate, since several passengers may be using the common air-to-ground link simultaneously. Second generation systems, like GSM, were originally designed for efficient delivery of voice services. UMTS networks are, on the contrary, designed from the beginning for flexible delivery of any type of service.

The current 3GPP specification (release 7) contains, among others, two significant extensions to the original 1999 release, which are known in the telecom industry as HSDPA (High Speed Downlink Packet Access) and HSUPA (High Speed Uplink Packet Access). HSDPA consists basically in introducing a new downlink transport channel known as HS-DSCH (High Speed Downlink Shared Channel) which is mapped onto the physical channel HS-PDSCH (HS-DSCH Physical Downlink Shared Channel), capable of transferring 960,000 physical (coded) bits per second (this is with 16QAM; if QPSK is used instead, 480,000 bps). Multicoding, that is, as-

1 Introduction

Assignment of several channelization codes to the same user, makes it possible for the network to allocate up to 15 HS-PDSCH physical channels to the same user (see Figure 1.3). Depending on the UE radio access capabilities (in this case, how many HS-PDSCH physical channels it can process simultaneously), up to 14.4 Mbps can be retrieved at the UE (7.2 Mbps with QPSK). It must be kept in mind, however, that this is a theoretical limit for the downlink physical channel bit rate. First, 16QAM will only be used if the propagation conditions are very good, typically when the user is close to the base station. Second, it does not seem reasonable to expect the network to assign all available HS-PDSCH physical channels (15) to the same user, except in the case that there is only one user in the cell in question (in our case, a single aircraft). But most importantly, more than half of the bits (usually around 60%) are not user bits: they are typically parity bits from channel coding, CRC (Cyclic Redundancy Check) bits, rate matching bits or control bits. Therefore, a more realistic figure may be obtained by considering QPSK, 5 channelization codes and the above-mentioned 40% factor, yielding a maximum downlink information data rate for the user in the vicinity of 1 Mbps ($0.48 \times 5 \times 0.4 = 0.96$ Mbps). In the case of an aircraft close to the base station, with no other aircraft in the cell consuming radio resources and/or generating multiple access interference, a possible though very unusual case, the aircraft could receive a few megabits per second ($0.96 \times 15 \times 0.4 = 5.76$ Mbps).

In an analogous way, HSUPA introduces the so-called E-DCH (Enhanced Dedicated Channel) uplink transport channel, which is in turn mapped onto the corresponding physical channel E-DPDCH (E-DCH Dedicated Physical Data Channel). In this case, the physical channel data rate limit is 5.76 Mbps and is obtained for a combination of spreading factors, as shown in Figure 1.3. A realistic figure may be obtained, for example, by considering a single E-DPDCH physical channel with spreading factor 4. Such a channel is capable of transferring 960 kbps (BPSK is always used in the uplink). Considering a factor of 40% as the ratio between user bits and physical bits results in a maximum uplink data rate around 384 kbps ($960 \times 1 \times 0.4 = 384$ kbps). If the physical channel has a spreading factor 2, the data rate doubles, i.e. 768 kbps.

This thesis is structured as follows. Chapter 2 presents a brief overview of the UMTS system architecture and some of the main aspects of WCDMA, such as power control and handover procedures. Chapter 3 concentrates on the idea of reproducing the cellular structure of UMTS in the airspace. It analyzes some aircraft specific constraints such as Doppler shift, propagation delay, interference and handover. Chapter 4 describes the model used to investigate the effect of interference generated by an aircraft on the ground infrastructure. Based on this model, we derive equations relating the size of the airspace cell to the transmit power increase of the terrestrial user, taking into account the radiation pattern of terrestrial base station antennas. Chapter 5 explains the architecture of the uplink WCDMA physical layer simulator implemented, describing the processing involved (channel coding, interleaving, spreading and scrambling). Chapter 6 presents the results of the link level simulations. This raw data is used in combination with the equations derived in Chapter 4 to provide a quantitative analysis of the performance degradation experienced by the terrestrial link. Chapter 7 draws the conclusions from this work and gives an outlook for future work.

Maximum physical channel bit rates with HSDPA/HSUPA



5.76 Mbps

UE (User Equipment \equiv Aircraft Equipment)

may transmit within a bandwidth of 5 MHz up to **5.76 Mbps** with HSUPA (E-DCH transport channel)

using 2x E-DPDCH (SF=2) + 2x E-DPDCH (SF=4)

HSUPA	High Speed Uplink Packet Access
E-DCH	Enhanced Dedicated Channel
E-DPDCH	Enhanced Dedicated Physical Data Channel

14.4 Mbps



NODE B (UMTS Base Station)

may transmit within a bandwidth of 5 MHz up to **14.4 Mbps** with HSDPA (HS-DSCH transport channel)

using 15x HS-PDSCH (SF=16) and 16QAM

HSDPA	High Speed Downlink Packet Access
HS-DSCH	High Speed Downlink Shared Channel
HS-PDSCH	High Speed Physical Downlink Shared Channel

Figure 1.3: Maximum physical channel bit rates in UMTS with HSDPA/HSUPA

1 Introduction

2 Overview of UMTS and WCDMA

This chapter presents a brief overview of UMTS and explains the main system design parameters related to the WCDMA air interface.

2.1 Summary of the main parameters in WCDMA

WCDMA is a Wideband Direct-Sequence Code Division Multiple Access (DS-CDMA) system, i.e. user information bits are spread over a wide bandwidth by multiplying the user data with quasi-random bits (called chips) derived from CDMA spreading codes. In order to support very high bit rates (up to 2 Mbps), the use of variable spreading factors and multicode connections is supported.

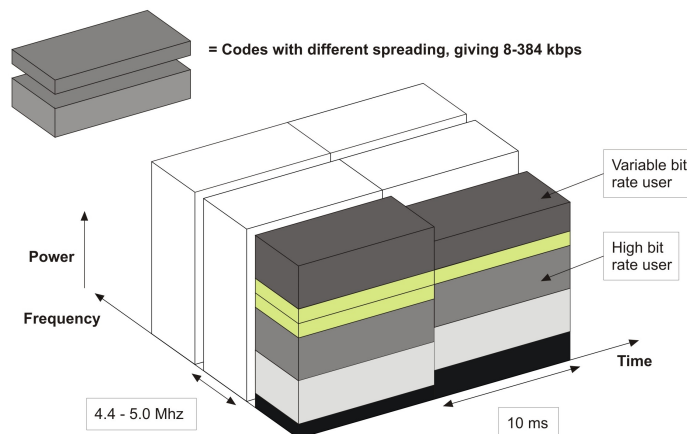


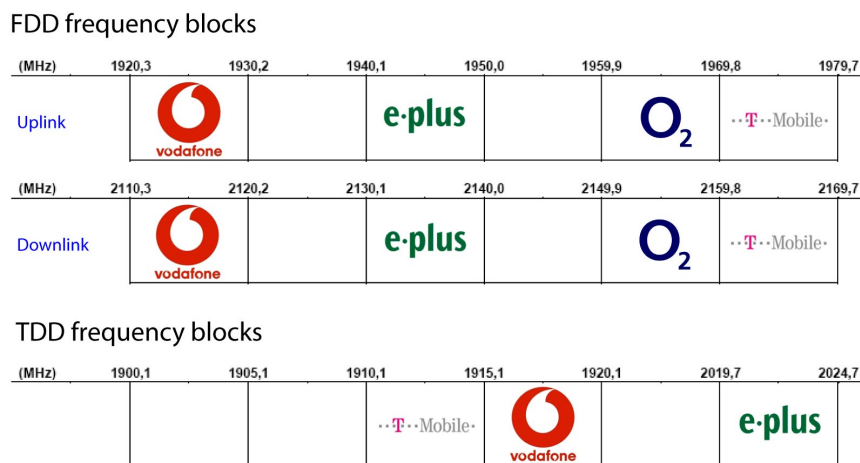
Figure 2.1: Allocation of bandwidth in WCDMA in the time-frequency-code space

As shown in Figure 2.1, the chip rate of 3.84 Mcps leads to a carrier bandwidth of approximately 5 MHz. DS-CDMA systems with a bandwidth of about 1 MHz, such as IS-95 are commonly referred to as narrowband CDMA systems. The inherently wide carrier bandwidth of WCDMA supports high user data rates and also certain performance benefits, such as increased multipath diversity. Subject to his operating license, the network operator can deploy multiple 5 MHz carriers to increase capacity, possibly in the form of hierarchical cell layers. Figure 2.2 shows the

2 Overview of UMTS and WCDMA

UMTS spectrum in Germany. Currently, there are four network operators providing UMTS services in FDD mode (T-Mobile, Vodafone, O₂ and E-Plus), each with a paired 10-MHz band, i.e. two channels.

UMTS frequency allocation in Germany



Source: Bundesnetzagentur (www.bundesnetzagentur.de)

Figure 2.2: UMTS frequency allocation in Germany

WCDMA also supports highly variable user data rates, in other words, the concept of obtaining Bandwidth on Demand (BoD) is well supported. The user data rate is kept constant during each 10 ms frame. However, the data capacity among the users can change from frame to frame. This fast radio capacity allocation will typically be controlled by the network to achieve optimum throughput for packet data services.

WCDMA supports two basic modes of operation: Frequency Division Duplex (FDD) and Time Division Duplex (TDD). In the FDD mode, separate 5 MHz carrier frequencies are used for the uplink and downlink respectively, whereas in the TDD only one 5 MHz is time shared between the uplink and the downlink.

WCDMA supports the operation of asynchronous base stations, so that, unlike in the synchronous IS-95 system, there is no need for a global time reference such as GPS. It also employs coherent detection on uplink and downlink based on the use of pilot symbols or common pilot. The WCDMA air interface has been crafted in such a way that advanced CDMA receiver concepts, such as multiuser detection and smart adaptive antennas, can be deployed by the network operator as a system option to increase capacity and or coverage. WCDMA is developed in conjunction with GSM. Therefore, handovers between GSM and WCDMA are supported in order to be able to leverage the GSM coverage for the introduction of WCDMA. The following sections explain

some important phenomena of UTRA.

2.2 Power Control

Tight and fast power control is perhaps the most important aspect in WCDMA, in particular on the uplink. Without it, a single overpowered mobile could block a whole cell. Below is a brief explanation of the power control concept. Mobile stations MS1 and MS2 operate within the same frequency, separable at the base station only by their respective spreading codes. It may happen that MS1 at the cell edge suffers a path loss, say, 70 dB above that of MS2, which is near the base station BS. If there were no mechanism for MS1 and MS2 to be power-controlled to the same level at the base station, MS2 could easily overshoot MS1 and thus block a large part of the cell, giving rise to the so-called near-far problem of CDMA. The optimum strategy in the sense of maximizing the capacity is to equalize the received power per bit of all mobile stations at all times.

While one can conceive open loop power control mechanisms that attempt to make a rough estimate of path loss by means of a downlink beacon signal, such a method would be too inaccurate. The prime reason for this is that the fast fading is essentially uncorrelated between uplink and downlink, due to the large frequency separation of the uplink and downlink bands of the WCDMA FDD mode. Open loop power control is, however, used in WCDMA, but only to provide a coarse initial power setting of the mobile station at the beginning of a connection.

The solution to power control in WCDMA is fast closed loop power control. In closed loop power control in the uplink, the base station performs frequent estimates of the received signal-to-interference ratio (SIR) and compares it to a target SIR. If the measured SIR is higher than the target SIR, the base station will command the mobile station to lower the power; if it is too low, it will command the mobile station to increase its power. This measure-command-react cycle is executed at a rate of 1500 times per second (1.5 kHz) for each mobile station and thus operates faster than any significant change of path loss could possibly happen and, indeed even faster than the speed of fast rayleigh fading for low to moderate mobile speeds. Thus, closed loop power control will prevent any power imbalance among all uplink signals received at the base station.

The same closed loop power control technique is also used on the downlink, though here the motivation is different: on the downlink there is no near-far problem due to the one-to-many scenario. All the signals within one cell originate from the one base station to all mobiles. It is, however, desirable to provide a marginal amount of additional power to the mobile stations at the cell edge, as they suffer from increased other-cell interference. Also on downlink a method of enhancing weak signals caused by Rayleigh fading with additional power is needed at low speeds when other error-correcting methods based on interleaving and error correcting code do not yet work effectively.

Closed loop power control commands the mobile station to use a transmit power proportional

2 Overview of UMTS and WCDMA

to the inverse of the received power (or SIR). Figure 2.3 illustrates the concept of closed loop power control in UMTS. Provided the mobile stations have enough head room to ramp the power up, only very little residual fading is left and the channel becomes an essentially non-fading channel as seen from the base station receiver. While this fading removal is highly desirable from the receiver point of view, it comes out at the expense of increased average transmit power at the transmitting end. This means that a mobile station in a deep fade, i.e. using a large transmission power, will cause increased interference to other cells.

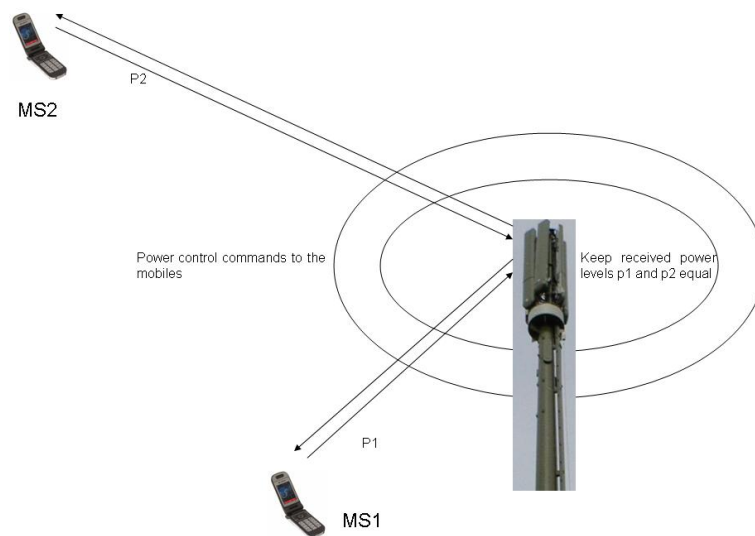


Figure 2.3: Closed loop Power control in WCDMA

Before leaving the area of closed loop power control, attention is drawn toward one more related control loop connected with it: outer loop power control. Outer loop power control adjusts the target SIR setpoint in the base station according to the needs of the individual radio link and aims at a constant quality, usually defined as a certain target bit error rate (BER) or block error rate (BLER), which depends on the mobile speed and the multipath profile. Now, if one were to set the target SIR setpoint for the worst case, i.e. high mobile speeds, one would waste much capacity for those connections at low speeds. Thus, the best strategy is to let the target SIR setpoint float around the minimum value that just fulfills the required target quality. The target SIR setpoint will change over time.

Outer loop control is typically implemented by having the base station tag each uplink user data with a frame reliability indicator, such as a CRC check result obtained during the decoding of that particular user data frame. Should the frame quality indicator indicate to the Radio Network Controller (RNC) that the transmission quality is decreasing, the RNC in turn will command the base station to increase the target SIR setpoint by a certain amount. The reason for having outer

loop control reside in the RNC is that this function should be performed after a possible soft handover combining.

2.3 Softer and soft handovers

During **softer handover**, a mobile station is in the overlapping cell coverage area of two adjacent sectors of a base station. The communication between mobile station and base station take place concurrently via two air interface channels, one for each sector separately. This requires the use of two separate codes in the downlink direction, so that the mobile station can distinguish the signals. The two signals are received in the mobile station by means of rake processing, very similar to multipath reception, except that the fingers need to generate the respective code for each sector for the appropriate despreading operation. Figure 2.4 shows the softer handover scenario.

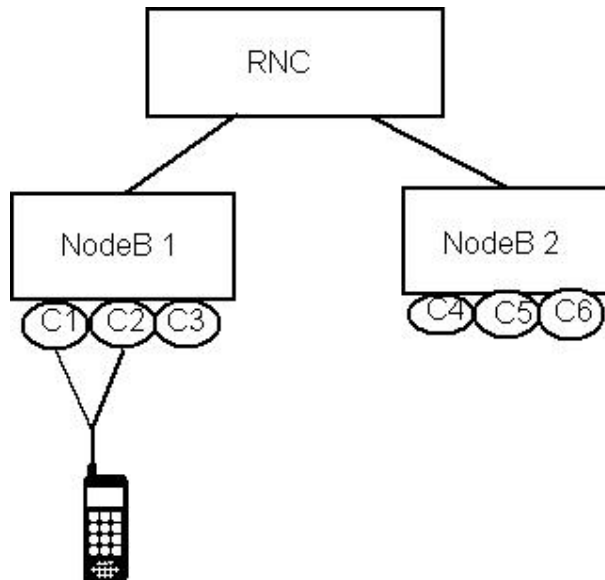


Figure 2.4: Softer Handover

In the uplink direction, a similar process takes place at the base station: the code channel of the mobile station is received in each sector, then routed to the same baseband rake receiver and the maximal ratio combined there in the usual way. During softer handover, only one power control loop per connection is active. Softer handover typically occurs in about 5-15 % of connections.

During **soft handover**, a mobile station is in the overlapping cell coverage area of two sectors belonging to two different base stations. As in softer handover, the communications between mobile station and base station take place concurrently via two air interface channels from each

2 Overview of UMTS and WCDMA

base station separately. As in softer handover, both channels (signals) are received at the mobile station by maximal ratio combining rake processing. Seen from the mobile, there are very few differences between softer and soft handover.

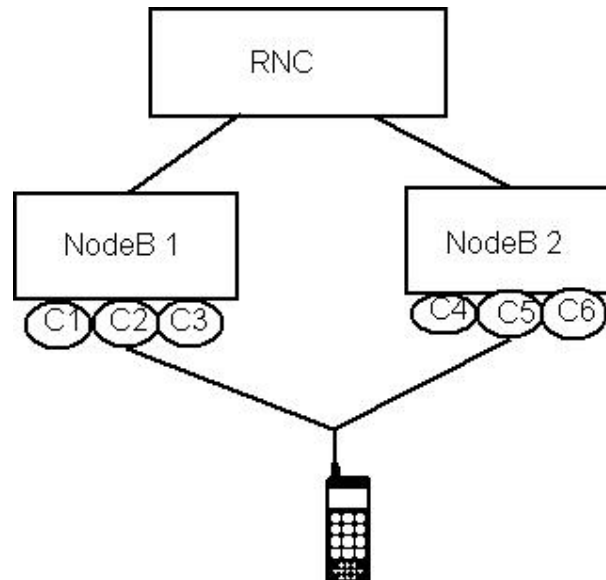


Figure 2.5: Soft Handover

However, in the uplink direction, soft handover differs significantly from softer handover: the code channel of the mobile station is received from both base stations, but the received data is then routed to the RNC for combining. This is typically done so that the same frame reliability indicator as provided for outer loop power control is used to select the better frame between the two possible candidates within the RNC. This selection takes place after each interleaving period, i.e. every 10-80 ms. Figure 2.5 shows the soft handover scenario.

During soft handover, two power control loops per connection are active, one for each base station. Soft handover occurs in 20-40 % of connections. To cater for soft handover connections, the following additional resources need to be provided by the system and must be considered in the planning phase:

- Additional rake receiver channels in the base stations.
- Additional transmission links between base stations and RNC.
- Additional rake fingers in the mobile stations.

We can also find that in UMTS soft and softer handover can take place in combination with each other. It is same as softer handover but in this case the cells belong to more than one nodeB and the combining is then done at the RNC. In general it is possible to have softer and soft handovers

simultaneously.

A more **complicated soft handover** would include a cell that belongs to a Node B in different RNC. In this case an I_{ur} connection is established with the drift RNC (RNC 2) and the data would be transferred to the Serving RNC (RNC 1) via I_{ur} connection. This is shown in Figure 2.6.

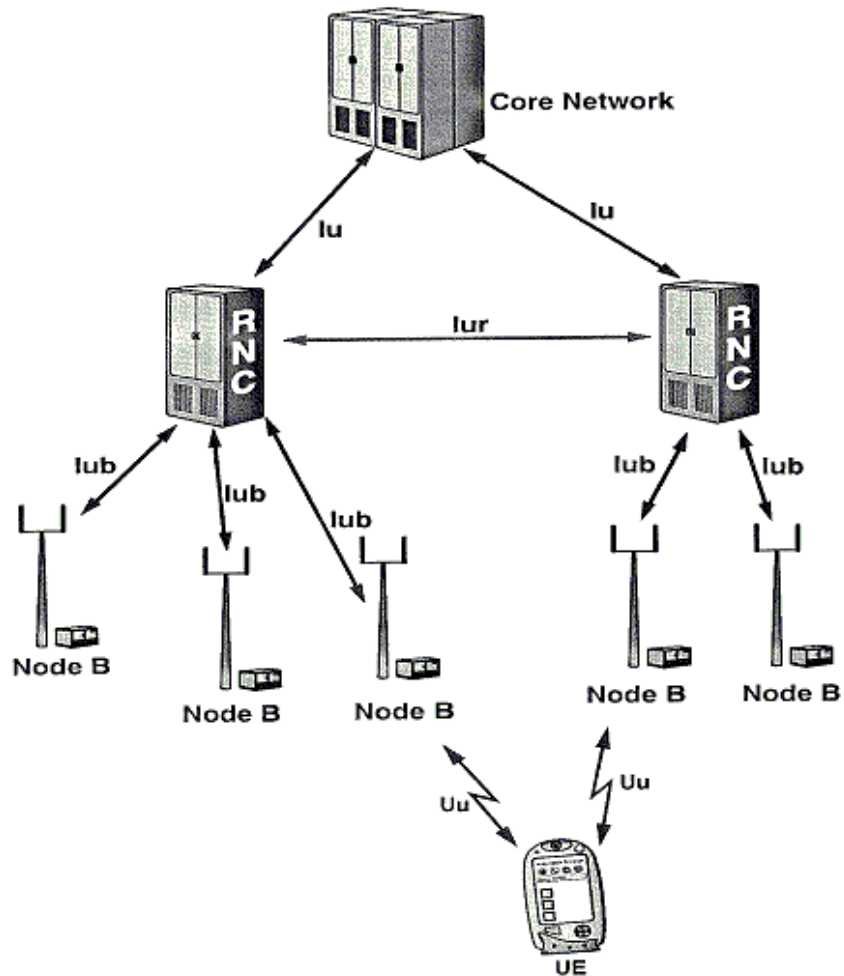


Figure 2.6: Inter-RNC soft handover

2.4 Radio Access Network Architecture

This section gives a broad view of the UMTS system architecture with a short introduction to the various functionalities of different network elements of the Radio Access Network.

2 Overview of UMTS and WCDMA

The UMTS system utilizes the same well-known architecture that has been used by all main second generation systems and even by some first generation systems. The UMTS system consists of logical network elements that each has a defined functionality. In the standards, network elements are defined at the logical level, but this quite often results in a similar physical implementation, especially since there are a number of open interfaces (for an interface to be ‘open’, the requirement is that it has been defined to such a detailed level that the equipment at the end points can be from different manufacturers). The network elements can be grouped based on similar functionality, or based on which sub-network they belong to. Functionally, the network elements are grouped into the Radio Access Network (RAN, UMTS Terrestrial RAN = UTRAN) that handles all radio-related functionality, and the Core network, which is responsible for switching and routing calls and data connections to external networks. To complete the system, the User Equipment (UE) that interfaces with the user and the radio interface is defined. The high level system architecture is shown in Figure 2.7.

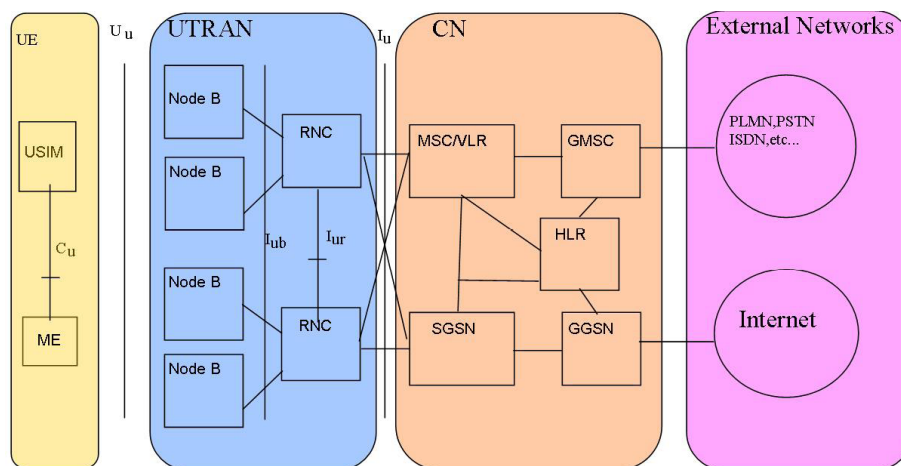


Figure 2.7: UMTS System Architecture

From a specification and standardization point of view, both UE and UTRAN consist of completely new protocols, the design of which is based on the needs of the new WCDMA radio technology. On the contrary, the definition of Core Network is adopted from GSM. This gives the system with new radio technology a global base of known and rugged CN technology that accelerates and facilitates its introduction, and enables such competitive advantages and global roaming.

Another way to group UMTS network elements is to divide them into sub networks. The UMTS system is modular in the sense that it is possible to have several network elements of the same type. In principle, the minimum requirement for a fully featured and operational network is to have at least one logical network element of each type. The possibility of having several entities of the same type allows the division of the UMTS system into sub-networks that are operational

either on their own or together with other sub networks and that they are distinguished from each other with unique identities. Such a sub network is called UMTS PLMN (Public Land Mobile Network), typically one PLMN is operated by a single operator and is connected other PLMN as well as to other types of network, such as ISDN, PSTN, the internet and so on. Figure 2.7 shows elements in a PLMN and in order to illustrate the connections, shows also connections to external networks.

A short introduction to all the elements is given below.

The UE consists of two parts:

The Mobile Equipment (ME) is the radio terminal used for radio communication over the U_u interface.

The UMTS Subscriber Identity Module (USIM) is a smartcard that holds the subscriber identity, performs authentication algorithms and stores authentication and encryption keys and some subscription information that is needed at the terminal.

UTRAN also consists of two distinct elements:

The Node B converts the data flow between the I_{ub} and U_u interfaces. It also participates in radio resource management.

The Radio Network Controller (RNC) owns and controls the radio resources in its domain (the Node B's connected to it). RNC is the service access point for all its services UTRAN provides the CN, for example, management of connections to the UE.

The main elements of the GSM CN are as follows:

HLR (Home Location Register) is a database located in the user's home system that stores the master copy of the user's service profile. The service profile consists of, for example, information on allowed services, forbidden roaming areas, and supplementary service information such as status of call forwarding and the call forwarding number. It is created when a new user subscribes to the system and remains stored as long as the subscription is active. For the purpose of routing incoming transaction to the UE (calls or short messages), the HLR also stores the UE location on the level of MSC/VLR and/or SGSN, i.e. on the level of the serving system.

MSC/VLR (Mobile Services Switching Center/Visitor Location Register) is the switch (MSC) and database (VLR) that serves the UE in its current location for Circuit Switched (CS) services. The MSC function is used to switch the CS transactions, and the VLR function holds a copy of the visiting user's service profile, as well as more precise information on the UE's location within the serving system. The part of the network that is accessed via the MSC/VLR is often referred to the CS domain. MSC also has a role in the early UE handling.

GMSC (Gate way MSC) is the switch at the point where UMTS PLMN is connected to external CS networks. All incoming and outgoing CS connections go through GMSC. SGSN (Serving GPRS Support Node) functionality is similar to that of MSC/VLR but is typically used for packet switched (PS) services. The part of the network that is accessed via the SGSN is often referred to

2 Overview of UMTS and WCDMA

as the PS domain. Similar to MSC, SGSN support is needed for the early UE handling operation. GGSN (Gateway GPRS Support Node) has functionality that is close to that of GMSC but is in relation to PS services.

The external networks can be divided into two groups:

CS Networks: These provide circuit switched connections, like existing telephony service. ISDN and PSTN are examples of CS networks.

PS networks: These provide connections for packet data services. The internet is one example of a PS network.

The UMTS standards are structured so that internal functionality of the network elements is not specified in detail. Instead, the interfaces between logical network elements have been defined. The following main open interfaces are specified:

C_u Interface: This is the electrical interface between the USIM smartcard and the ME. The interface follows a standard format for smartcards.

U_u Interface: This is the WCDMA radio interface. The U_u interface through which the UE accesses the fixed point point of the system and is probably the most important open interface in UMTS. There are likely to be many more UE manufacturers than manufacturers of fixed networks elements.

I_u Interface: This connects UTRAN to CN. Similarly, to the corresponding interfaces in GSM, a (Circuit Switched) and G_b (Packet Switched), the open I_u interface gives UMTS operators the possibility of acquiring UTRAN and CN from different manufacturers. The enabled competition in this area has been one of the success factors of GSM.

I_{ur} Interface: This is the open interface that allows soft handover between RNC's from different manufacturers and therefore complements the open I_u interface.

I_{ub} Interface: The I_{ub} connects a Node B and an RNC. UMTS is the first commercial mobile telephony system where the controller base station interface is standardized as a fully open interface. Like the other open interfaces, open I_{ub} is expected to further motivate competition between manufacturers in this area. It is likely that the new manufacturers concentrating exclusively on Node B's will enter the market.

2.5 Services and Functions of the Physical Layer

The Physical Layer (Layer 1) is the lowest layer in the Open System Interconnection (OSI) Reference Model and it supports all functions required for the transmission of bit streams on the physical medium. The physical layer offers data transport services to higher layers. The access to these services is through the use of transport channels via the MAC (Medium Access Control) sub layer. The characteristics of a transport channel are defined by its transport format (or format set), specifying the physical layer processing to be applied to the transport channel in question, such as convolutional channel coding and interleaving and any service specific rate matching as needed.

The physical layer operates exactly according to the L1 radio frame timing. A transport block is defined as the data accepted by the physical layer to be jointly CRC protected. The transmission block timing is then tied exactly to the TTI timing, e.g. every transmission block is generated precisely every TTI.

A UE can set up multiple transport channels simultaneously, each having own transport characteristics (e.g. offering different error correction capability). Each transport channel can be used for information stream transfer of one radio bearer or for layer 2 and higher layer signalling messages. The multiplexing of transport channels onto the same or different physical channels is carried out by L1.

2.5.1 Overview of L1 functions

The Physical layer performs the following main functions:

- FEC encoding/decoding of transport channels
- Measurements and indication to higher layers (e.g. FER, SIR, interference power, transmission power, etc...)
- Macro diversity distribution/combining and soft handover execution.
- Error detection on transport channels.
- Multiplexing of transport channels and demultiplexing of coded composite transport channels.
- Rate Matching
- Mapping coded composite transport channels on physical channels.
- Modulation and spreading/demodulation and despreading of physical channels.
- Frequency and time (chip, bit, slot, frame) synchronisation.
- Closed-loop power control.
- Power weighting and combining of physical channels.
- RF processing.
- Support of uplink synchronisation (TDD only)
- Timing advance on uplink channels (TDD only)

2 Overview of UMTS and WCDMA

3 Analysis of aircraft specific constraints

In this chapter, we consider the idea of reproducing the cellular structure of terrestrial UMTS in the airspace, with special skyward antennas. Figure 3.1 illustrates this idea.



Figure 3.1: Illustration of airspace cell structure

In order to determine an appropriate cell size for the system, it is necessary to consider the following facts:

- The aircraft location distribution and density will impose a certain traffic demand on the network for a given cell size. If cells are too large, too many aircraft will have to be handled by the same Node B, reducing performance because of limited available throughput at the Node B.
- Having too many aircraft in the same cell reduces performance also due to interference among aircraft, since the base station receiver is not able to perfectly separate signals coming from different aircraft, owing to the non-orthogonality of scrambling codes.
- Link budget limits the maximum distance between the aircraft and the Node B for a given maximum transmits power and receiver sensitivity.

3 Analysis of aircraft specific constraints

- Existing terrestrial base station antennas typically have some skyward side lobes. If aircraft transmit at the same frequencies as mobile terminals on the ground, the performance of the terrestrial network in the uplink will be degraded. If aircraft cells are too large, the transmit power at the aircraft will necessarily be very high, making this degradation intolerable.
- Aircraft flight speed is relatively high (around 900 km/h, or 15 km/min). If cells are too small, handovers will occur too often.
- The idea is to cover a reasonably large area (Europe) while minimizing deployment costs. If cells are too small, many base stations will be required, making the system economically unviable.

It is therefore necessary to find a compromise between these criteria. Since we do not have at our disposal any information on aircraft location distribution for this study, it is difficult to estimate a reasonable figure for the cell size of the system. Nevertheless, we have considered a cell radius of 50 km as a minimum, following the aircraft flight speed criterion. Figure 3.2 shows the probability density function of the flight path length within the same cell, assuming straight flight trajectories for all aircraft and uniformly distributed directions of flight (the derivation is given in C). It can be shown that for a cell radius of 50 km, two thirds of the aircraft remain within the same cell at least a few minutes (3 to 6 minutes, approximately).

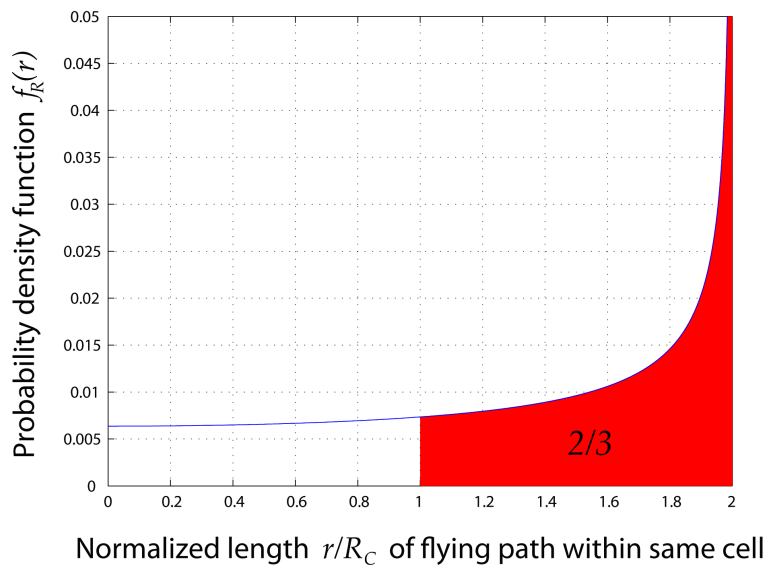


Figure 3.2: Probability density function of flight path length within same cell

The idea of extending UMTS coverage to the airspace, with every aircraft seen as an additional mobile station from the ground infrastructure, implies a geometrical transformation that affects the air interface between UE and Node B. Usually, mobile stations are located on the ground and move relatively slowly with respect to the wireless infrastructure. Within this study, mobile stations (aircraft) are located several kilometers above ground, and move at much higher speeds.

Figure 3.3 shows the worst case scenario. The mobile station flies at an altitude h with velocity v , and is located at the central point between two adjacent base stations. At this location, the signal experiences the longest propagation delay and the greatest Doppler shift, as seen from both base stations. In addition, it is at this location (or in the vicinity) that the mobile station attempts to execute a soft handover (macrodiversity), that is, establish a new radio link with the approaching base station without releasing the current radio link. Moreover, this location is furthest from the base station within the cell, so that the mobile station must transmit with full power to compensate for a greater path loss, generating greater interference in the existing terrestrial network. Each of these aspects will be dealt with separately in the subsequent sections.

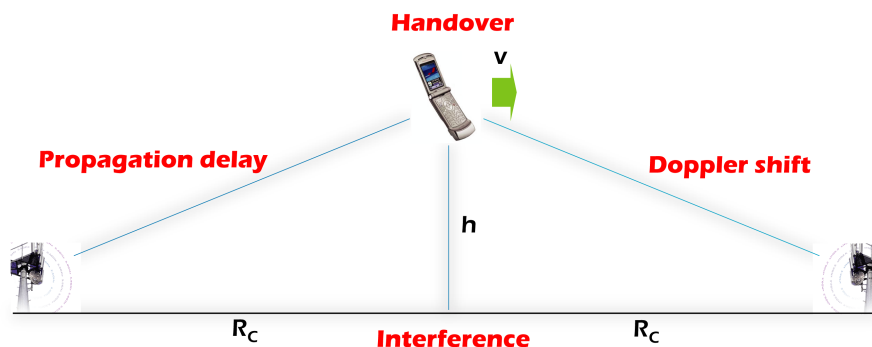


Figure 3.3: Worstcase scenario

3.1 Propagation delay

In WCDMA, frames are of length 38400 chips (10 ms) and consist of 15 slots, each of length 2560 chips. With every new slot, the transmit power is adjusted (both at the base station and at the mobile station), according to the power control command received. This is known as inner loop power control, or fast power control, since it takes place 1500 times per second. Given a chip rate of 3.84 Mcps, having a cell radius of 50 km implies that mobile stations at the cell boundary experience a propagation delay of 640 chips.

There seem to be no specific constraints on the maximum propagation delay in the UTRA FDD radio access mode. The equations in Figure 3.4 show the definition of propagation delay as given by 3GPP, where PRACH stands for Physical Random Access Channel and is an uplink physical channel used for random access.

One of the key services provided by the air interface physical layer is the measurement of various quantities which are used to trigger or perform a multitude of functions. Both the UE and the UTRAN are required to perform a variety of measurements. One of these is precisely the PRACH propagation delay measurement. Figure 3.5 shows the mapping specified for reporting

3 Analysis of aircraft specific constraints

Propagation delay is defined as one-way propagation delay as measured during PRACH access.

Propagation delay = $(T_{RX} - T_{TX} - 2560)/2$, where:

T_{TX} = The transmission time of AICH access slot ($n-2$ -AICH transmission timing), where $0 \leq (n-2$ -AICH Transmission Timing) ≤ 14 and AICH_Transmission_Timing can have values 0 or 1. The reference point for T_{TX} shall be the Tx antenna connector.

T_{RX} = The time of reception of the beginning (the first detected path, in time) of the PRACH message from the UE at PRACH access slot n . The reference point for T_{RX} shall be the Rx antenna connector.

Figure 3.4: Propagation delay definition according to 3GPP

this measurement. The last value is 765 chips, suggesting that a distance of 50 km could in principle be tolerable. Another indication that propagation delay does not seem to be critical in FDD

PRACH Propagation delay measurement report mapping

The PRACH Propagation delay reporting range is from 0 ... 765 chip.

Reported value	Measured quantity value	Unit
PROP_DELAY_000	$0 \leq$ PRACH Propagation delay < 3	chip
PROP_DELAY_001	$3 \leq$ PRACH Propagation delay < 6	chip
PROP_DELAY_002	$6 \leq$ PRACH Propagation delay < 9	chip
...
PROP_DELAY_252	$756 \leq$ PRACH Propagation delay < 759	chip
PROP_DELAY_253	$759 \leq$ PRACH Propagation delay < 762	chip
PROP_DELAY_254	$762 \leq$ PRACH Propagation delay < 765	chip
PROP_DELAY_255	$765 \leq$ PRACH Propagation delay	chip

Figure 3.5: PRACH propagation delay measurement report mapping

is shown in Figure 3.6 figure.

Transmit Power Control (TPC) commands are sent in both directions after measuring the received signal-to-interference ratio (SIR) by means of pilot bits known at both ends of the link. If the user is close to the base station, propagation delay is low and transmitters at both ends are able to respond to the TPC command in the next slot. However, as indicated in the red line below the figure 3.6, "if there is not enough time for UTRAN to respond to the TPC, the action can be delayed until the next slot."

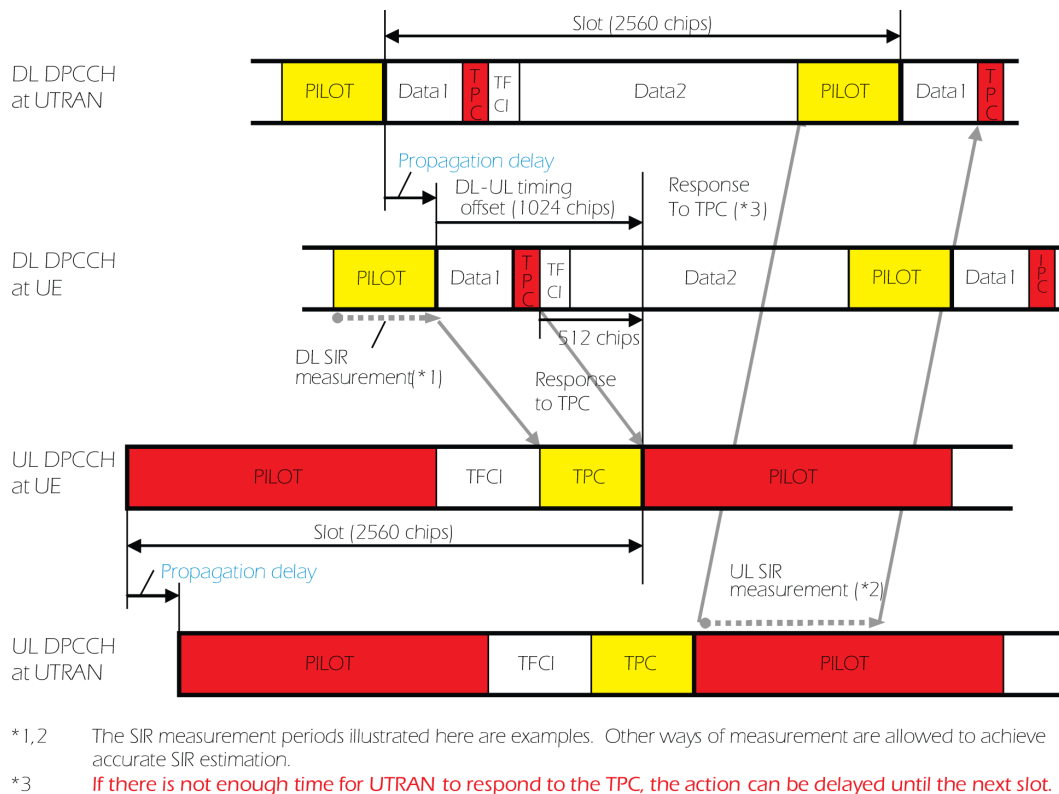


Figure 3.6: Transmit Power Control Timing

3.2 Doppler shift

Aircraft fly usually at speeds around 900 km/h (15 km/min). This means signals transmitted and received from the aircraft will suffer a significantly greater Doppler frequency shift as mobile terminals on the ground, which move at much lower speeds. Figure 3.7 shows the evolution of the Doppler shift of the signal received at the aircraft as it flies by over the base station. The closer the aircraft flies by over the base station, the sharper the variation of Doppler shift. The maximum shift is experienced when the aircraft is far from the base station, and is approximately 2 kHz for typical aircraft cruising speeds.

In WCDMA, base stations use a very accurate local oscillator at the transmitter, so that the difference in carrier frequency between two base stations is negligible. This accuracy requirement is specified by 3GPP as follows: "The modulated carrier frequency of the base station shall be accurate to within ± 0.05 ppm." At a carrier frequency of 2 GHz, this means the maximum difference in carrier frequency between any pair of base stations is 200 Hz.

The mobile terminals use a frequency acquisition circuit to syntonize accurately to the received frequency from the base station. In this case, the accuracy requirement is specified as follows:

3 Analysis of aircraft specific constraints

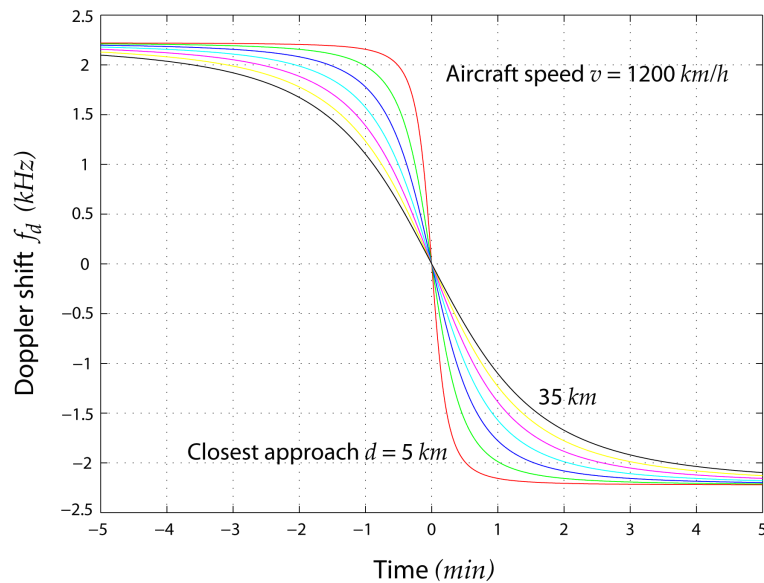


Figure 3.7: Evolution of Doppler shift as aircraft flies by over base station

"The UE modulated carrier frequency shall be accurate to within ± 0.1 ppm compared to the carrier frequency received from the Node B." This accuracy is equivalent to ± 200 Hz. However, the received signal suffers a certain Doppler shift, so that the mobile terminal synchronizes to a shifted frequency. In current terrestrial networks, this shift is in the range of a few hundred Hertz, but in the case of aircraft it could reach up to 2 kHz. Moreover, the transmitted signal from the terminal (which is itself already shifted) suffers an additional shift as seen from the base station receiver. This is illustrated in Figure 3.8

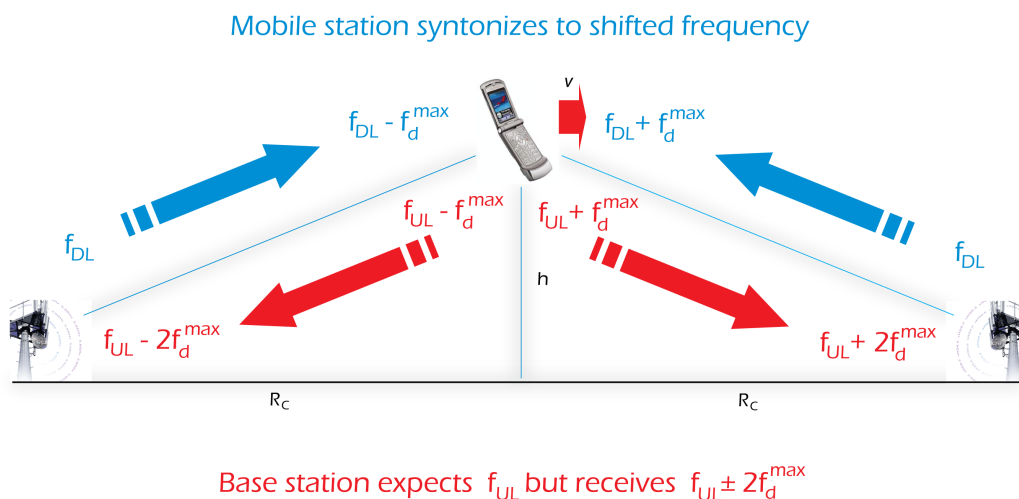


Figure 3.8: Doppler shift

This causes basically two problems

- The base station receives from many users simultaneously, each moving relative to the base station with a different speed. This means the base station receives a composite signal with different frequencies, around the nominal uplink carrier frequency it expects. In current networks, these frequencies are at most a few hundred Hertz away from the center frequency, but in the case of aircraft this frequency deviation can be up to ± 4 kHz. However, the base station performs frequency syntonization independently for each user, so this should not be of too much concern.
- The mobile terminal attempts to execute a soft handover when the signal from a neighboring cell becomes large enough. The signal received from the cell where the terminal is currently camped and the signal received from the neighboring cell may have different shifts, e.g. if the terminal is moving along the line joining both base stations at high speed. This means the terminal receives two signals at slightly different frequencies, but must be able to downconvert them with a single local oscillator. If the difference in frequency between the signals is too large, e.g. in the case of an aircraft attempting to perform a soft handover (4 kHz), the terminal receiver might not be able to execute soft handover. This is a subject for further study.

3.3 Handover

In current terrestrial WCDMA networks, terminals perform different kinds of handover procedures as they move from one spot to the other. These procedures involve both the terminal and the network. Since WCDMA has a frequency reuse of 1, i.e. all cells transmit/receive at the same frequency, most handovers do not involve a frequency switch in the terminal receiver. Hard handovers do occur occasionally, e.g. between different network operators. Soft handover consists basically in establishing a new radio link with another cell without releasing the current one. Thus, one terminal may have several radio links simultaneously to the network. This is also referred to as macrodiversity. The maximum number of radio links a terminal can handle is determined by its radio access capabilities.

Soft handover involves at least two cells. These cells may belong to the same Node B, in which case the procedure is called softer handover. If the cells belong to different Node Bs, but these Node Bs are managed by the same Radio Network Controller (RNC), the procedure is referred to as intra-RNC soft handover. In UMTS, as opposed to GSM, there is also the possibility to perform a soft handover even between cells whose Node Bs belong to different RNCs, thanks to the so-called I_{ur} interface existing between both RNCs.

In the airspace cellular system investigated in this study, UTRAN access points are expected to be relatively far apart from each other compared to the terrestrial case, since cells are much larger. Therefore, adjacent cells will be managed with all probability by different RNCs. These

3 Analysis of aircraft specific constraints

RNCs should implement this I_{ur} interface in order for aircraft to be able to perform soft handover. Figure 3.9 shows an excerpt from the 3GPP I_{ur} interface specification. In principle, any RNC is capable of addressing any other RNC within the PLMN for establishing a signaling or user data bearer over I_{ur} .

Addressing of RNSs over the Iur Interface

- For an RRC connection using a dedicated channel or for a UE using F-DPCH in the downlink, the Iur standard shall allow the addition / deletion of radio links supported by cells belonging to any RNS within the PLMN.
- The specification of the Iur interface shall allow an RNC to address any other RNC within the PLMN for establishing a signalling bearer over Iur.
- The specification of the Iur interface shall allow an RNC to address any other RNC within the PLMN for establishing user data bearers for Iur data streams.

RNSAP shall allow different kinds of addressing schemes to be used for the signalling bearer.

Figure 3.9: Excerpt from 3GPP I_{ur} interface specification

3.4 Interference

In WCDMA, each source (base station or mobile terminal) uses a different scrambling sequence for transmission, so that the receiver can separate signals coming from different sources (or select the signal from the desired source) by descrambling the received composite signal with the corresponding scrambling sequence. However, these sequences are not completely orthogonal, but rather quasi-orthogonal. This means there is always a certain amount of interference at the receiver. In the uplink (base station receives), the greater the number of users in the cell, the greater the interference experienced by each of them. This imposes a limit on the maximum number of users per cell. In the downlink, the mobile terminal receives signals from several base stations. However, thanks to macrodiversity (soft handover), this can be taken advantage of, minimizing so-called inter-cell interference. Indeed, WCDMA is an uplink-limited system. In the case of aircraft, these phenomena are described in the subsequent sections.

3.4.1 Forward link

In the forward link, aircraft base stations transmit and aircraft receive. As mentioned above, an aircraft will receive signals from several base stations, and will try to take advantage of this by means of macrodiversity, that is, by establishing additional radio links with base stations from which the received signal level is high enough. However, there are certain limitations on this procedure. For example, the relative delays among the different radio links constituting the radio link set must be within a certain time constraint. Whether this procedure works in a line-of-sight

environment (with no fading) remains to be investigated. Inter-cell interference could play an important role due to the line-of-sight nature of all links in the system.

If terrestrial frequencies are used, an additional problem arises. Some existing terrestrial base station antennas radiate partially skywards. The aircraft would therefore receive a significant amount of interference from these antennas, even at 10 km altitude, since there is line of sight. This could in principle be overcome by allowing a greater maximum transmit power at the aircraft base stations. Power control would ensure that signal-to-interference ratio at the receiver is high enough for the required performance.

3.4.2 Reverse Link

In the reverse link, aircraft transmit and aircraft base stations receive. Again, a base station will receive a composite signal from several aircraft. If the number of aircraft grows, the performance will become worse due to the non-orthogonality of the scrambling sequences. Power control will react to this phenomenon and have users increase their power. Users at the cell boundary, not being able to increase their any more, will lose their connection. This dependency between the number of users and the cell size is known as cell breathing, and should be taken into account to avoid coverage gaps in high density scenarios.

If terrestrial frequencies are used, existing terrestrial base stations will also receive the composite signal from aircraft, since they usually have a few skyward lobes. Power control will have mobile terminals increase their power to maintain the target signal-to-interference ratio, but users on the cell boundary won't be able to increase their power any more, so they will lose their connection. In other words, the cell will shrink, possibly giving rise to coverage gaps.

3 Analysis of aircraft specific constraints

4 Air-to-ground link model

4.1 Concept description

In this section, we intend to show the relationship between the maximum allowable airspace cell radius (within which the aircraft link exhibits the desired performance) and the cost in terms of transmit power increase required at the mobile terminal in order to maintain the performance of the terrestrial link in presence of interference from the aircraft at the base station receiver. In order to do so, we will use the raw data obtained by conducting the simulations using the simulator that will be described in the chapter 5 and a few theoretical formulae that will be derived next.

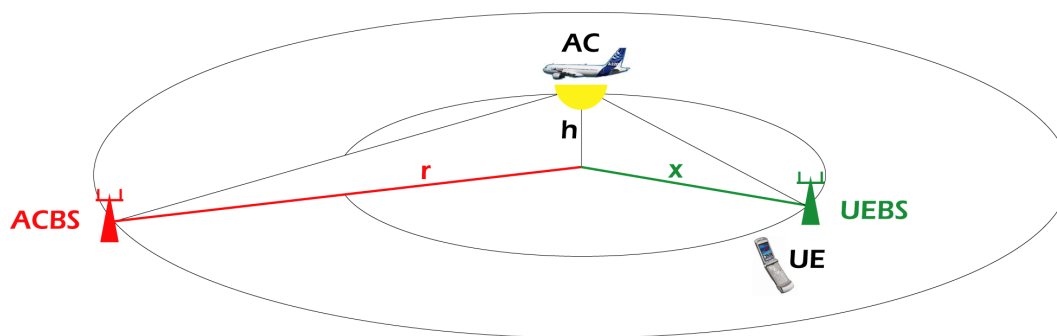


Figure 4.1: Geometry involved in the terrestrial and aircraft components

Figure 4.1 shows the scenario used for analysis. We have assumed a simplified scenario consisting of one mobile terminal (UE), in the cell, one aircraft (AC), one User Equipment (UE) base station (UEBS) and one aircraft (AC) base station (ACBS). The performance of the UEBS is degraded due to the presence of interference from the aircraft which will be explained in the following sections. Now we would like to derive the equations that would relate aircraft cell radius and the required user equipment (UE) power increase.

The required power at the receiver (be it the ACBS or UEBS receiver) for a block error rate BLER in presence of a level of interference given by the signal-to-interference ratio SIR can be computed as

$$P_{R,req} = \frac{E_b}{N_0} (BLER, SIR) + 10 \log_{10} N_0 + 10 \log_{10} R \quad (4.1)$$

4 Air-to-ground link model

where N_0 is the noise power spectral density and R is the user data rate (at the MAC-PHY reference point).

On the other hand, the actual received power is obtained from the link budget equation

$$P_R = P_T + G_T - L_{FS} + G_R \quad (4.2)$$

where P_T and P_R are the transmit and receive powers, G_T and G_R are the transmit and receive antenna gains and L_{FS} is the free space loss, all in logarithmic units. Free space loss is computed as

$$L_{FS}(d) = 32.44 + 20\log_{10}f + 10\log_{10}(h^2 + d^2) \quad (4.3)$$

for a carrier frequency f , a flight altitude h and a horizontal distance d .

The tolerable interference level at the UEBS receiver can be expressed as

$$I = P_{R,req}^{UEBS} - SIR_{UE} \quad (4.4)$$

where SIR_{UE} is the same as used to compute $P_{R,req}$ at the UEBS, according to 4.1. On the other hand, the actual interference seen by the UEBS from the aircraft is given by

$$I = P_T^{AC} + G_T^{AC}(\theta_{UEBS}, \phi_{UEBS}) - L_{FS}(x) + G_R^{UEBS}(\theta_{AC}, \phi_{AC}) \quad (4.5)$$

where x is the horizontal distance from the aircraft to the UEBS.

Now, the aircraft link performance requirement can be written as

$$P_R^{ACBS} \geq P_{R,req}^{ACBS} \quad (4.6)$$

Substituting equation 4.1 and equation 4.2 in equation 4.6 we obtain

4.1 Concept description

$$P_T^{AC} + G_T^{AC}(\theta_{ACBS}, \phi_{ACBS}) - L_{FS}(r) + G_R^{ACBS}(\theta'_{AC}, \phi'_{AC}) \geq \quad (4.7)$$

$$\frac{E_b}{N_0}(BLER_{AC}, SIR_{AC}) + 10\log_{10}N_0^{ACBS} + 10\log_{10}R_{AC}$$

where r is the horizontal distance from the aircraft to the ACBS. Substituting the tolerable aircraft transmit power P_T^{AC} from equation 4.5 (where the interference in equation 4.5 is given by equation 4.4. The required receive power at the UEBS $P_{R,req}^{UEBS}$ in equation 4.4 can be obtained in turn by applying the definition given in equation 4.1) into the equation 4.8, by defining

$$G = G_T^{AC}(\theta_{UEBS}, \phi_{UEBS}) - G_R^{UEBS}(\theta_{AC}, \phi_{AC}) + G_T^{AC}(\theta_{ACBS}, \phi_{ACBS}) + G_R^{ACBS}(\theta'_{AC}, \phi'_{AC})$$

and assuming $N_0^{ACBS} = N_0^{UEBS}$, yeilds

$$10\log_{10}(h^2 + r^2) \leq \frac{E_b}{N_0}(BLER_{UE}, SIR_{UE}) - \frac{E_b}{N_0}(BLER_{AC}, SIR_{AC}) + 10\log_{10}\frac{R_{UE}}{R_{AC}} \quad (4.8)$$

$$-SIR_{UE} + 10\log_{10}(h^2 + x^2) - G$$

This inequation allows us to obtain the maximum horizontal distance r between AC and ACBS within which the desired aircraft link performance is guaranteed as a function of the required UE power increase for the terrestrial link to maintain its performance. We can see this maximum distance r as the maximum cell radius of the aircraft cellular system, denoted by R_C^{max} . Simplifying terms we get

$$R_C^{max} = \min \left[Re \left(h \left(\frac{R_{UE}}{R_{AC}} \text{cosec}^2(\theta_{AC}) * 10^{\frac{E_b}{N_0}(BLER_{UE}, SIR_{UE}) - \frac{E_b}{N_0}(BLER_{AC}, SIR_{AC}) - SIR_{UE} - G}{10}} - 1 \right)^{\frac{1}{2}} \right) \right] \quad (4.9)$$

By defining

$$\alpha = \min_{\substack{\theta_{UEBS} \quad \phi_{UEBS} \\ \theta_{ACBS} \quad \phi_{ACBS} \\ \theta_{AC} \quad \phi_{AC} \\ \theta'_{AC} \quad \phi'_{AC}}} \left[\text{cosec}^2(\theta_{AC}) \frac{G_T^{AC}(\theta_{ACBS}, \phi_{ACBS})G_R^{ACBS}(\theta'_{AC}, \phi'_{AC})}{G_T^{AC}(\theta_{UEBS}, \phi_{UEBS})G_R^{UEBS}(\theta_{AC}, \phi_{AC})} \right] \quad (4.10)$$

4 Air-to-ground link model

and assuming the argument of the square root in equation 4.9 is positive, the maximum cell radius when a single aircraft is present ($SIR_{AC} = \infty$)

$$R_C^{max} = h \left[\alpha \frac{R_{UE}}{R_{AC}} * 10^{\frac{\Delta P_T^{UE} + \frac{E_b}{N_0}(BLER_{UE}, \infty) - \frac{E_b}{N_0}(BLER_{AC}, \infty) - SIR_{UE}}{10}} - 1 \right]^{\frac{1}{2}} \quad (4.11)$$

We can particularize this formula for hemispheric antenna patterns at AC and ACBS, as well considering the worst case UEBS azimuth angle, by setting

$$G_T^{AC}(\theta, \phi) = G_T^{AC} = 3dB_i$$

$$G_R^{ACBS}(\theta, \phi) = G_R^{ACBS} = 3dB_i$$

$$G_R^{UEBS}(\theta, \phi) = G_R^{UEBS}(\theta)$$

Substituting the above antenna patterns into equation 4.10, we get a simplified expression for α

$$\alpha = \min_{\theta} \left[\frac{2 \cos^2(\theta)}{G_R^{UEBS}(\theta)} \right] \quad (4.12)$$

Moreover, if both UE and AC have the same data rate and performance requirement, simplifying equation 4.11 yields

$$R_c^{max} = h \left[\alpha * 10^{\frac{\Delta P_T^{UE} - SIR_{UE}}{10}} - 1 \right]^{\frac{1}{2}} \quad (4.13)$$

As this formula 4.13 indicates, the maximum cell radius grows linearly with flight altitude and has approximately a square-root dependency with the power increase at the mobile terminal.

4.2 Base station antenna study

How much interference an aircraft transmitting at UMTS frequencies generates on a terrestrial base station depends basically on:

- the skyward receive pattern of the base station, and

- the degree of quasi-orthogonality of the scrambling sequences used by mobile terminals and aircraft.

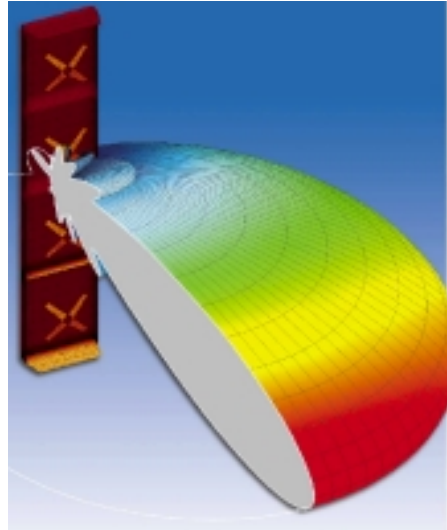


Figure 4.2: Typical directional pattern of a base station panel antenna for mobile communications

This section is dedicated to the first item. Figure 4.2 shows the three-dimensional radiation pattern of a typical base station panel antenna for mobile communications. The level of interference received at the base station will vary depending on the position of the aircraft relative to the antenna. For example, if the aircraft is behind the antenna, interference is expected to be relatively low, whereas directly in front of the main lobe, interference may increase significantly. Since most antennas are directional in azimuth, the worst scenario is chosen to be at 0° azimuth, seen in grey in Figure 4.2. Since there are many antennas on the ground within reach of the aircraft signal, some of them will be pointing in the direction of the aircraft (in azimuth), wherever the aircraft is. Interference at the base station can be estimated according to the formula shown in Figure 4.3. Note: The processing gain PG is considered in order to obtain an estimate of the interference level after chip processing at the WCDMA RAKE receiver. Applying this formula to a selection of typical base station antenna patterns obtained from a renowned mobile communications antenna manufacturer, we get the graphs shown in Figure 4.4.

As seen from the figures the first antenna (top left) presents significant skyward side lobes, particularly for high electrical down tilts. The other two antennas exhibit skyward side lobes with smaller beamwidths. However, the most critical part of the pattern as regards interference from aircraft seems to be the main lobe, especially when no down tilt is used at the antenna. Most antennas probably won't receive much signal from the zenith, but they will definitely receive with a high gain from a horizontal elevation angle. This is a crucial factor in determining the feasibility of an aircraft component in the UMTS licensed band.

4 Air-to-ground link model

$$I = P_T + G_T - FSL + G_R - PG$$

I (dBm)	Interference power at receiver
P_T (dBm)	Transmit power
G_T (dB)	Transmit gain
FSL (dB)	Free space loss
G_R (dB)	Receive gain
PG (dB)	Processing gain

Worst case values

33 dBm (power class 1)
3 dB (hemispheric)
various receive BS antennas
6 dB (SF=4)

$$FSL = 32.44 + 10\log(h^2 + r^2) + 20\log(f_{UL})$$

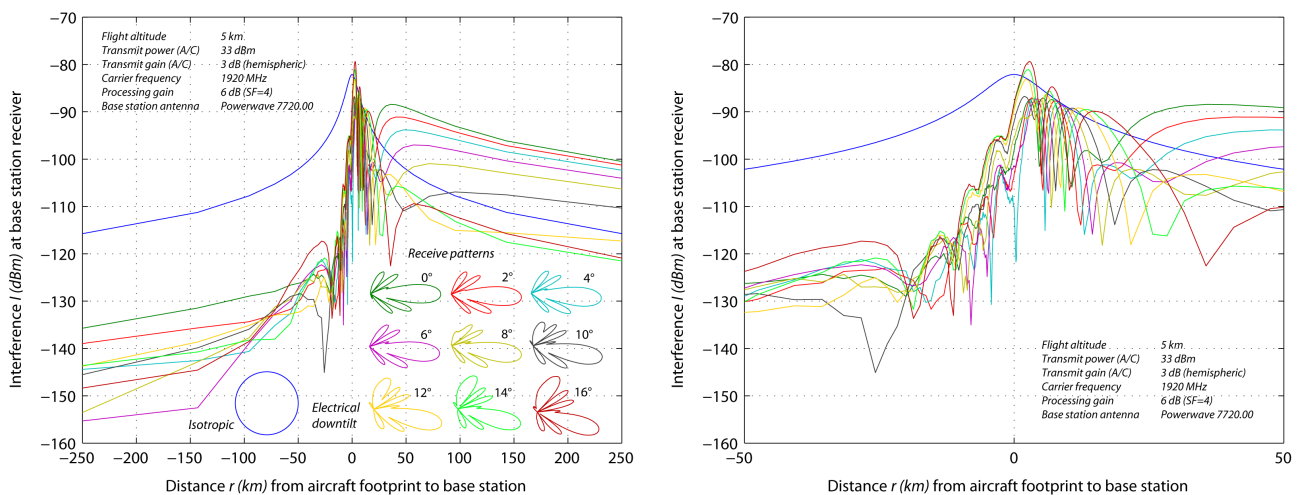
$$PG = 10\log(SF)$$

h (km)	Flight altitude	5 km
r (km)	Distance from aircraft footprint to BS	
f_{UL} (MHz)	Reverse link carrier frequency	1920 MHz
SF	Spreading factor of desired user signal	4

Worst case interference

$$I = -68.11 - 10\log(25 + r^2) + G_R$$

Figure 4.3: Interference estimation formula



4.2 Base station antenna study

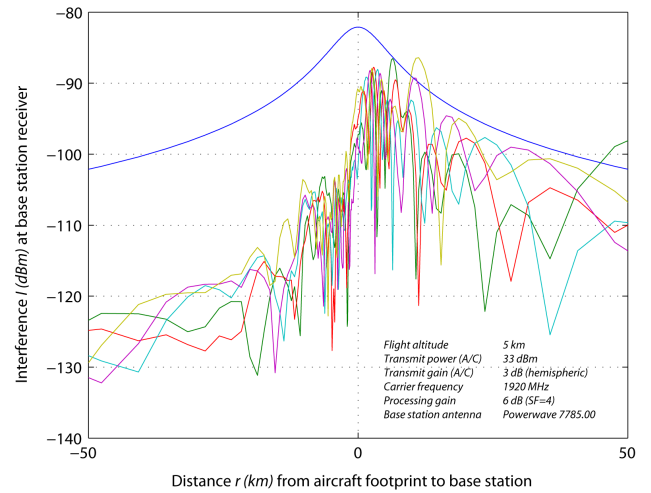
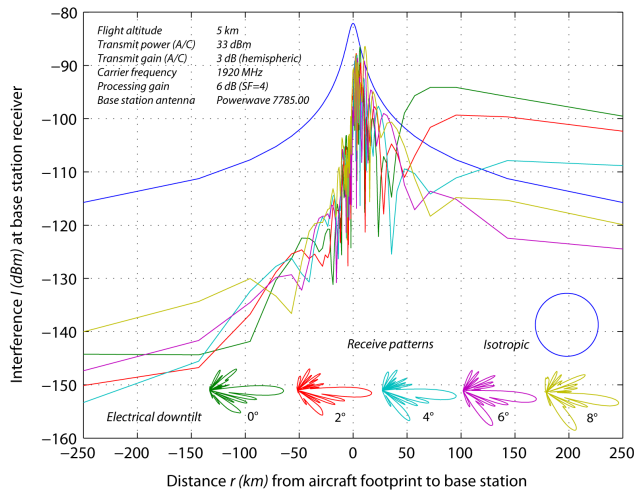
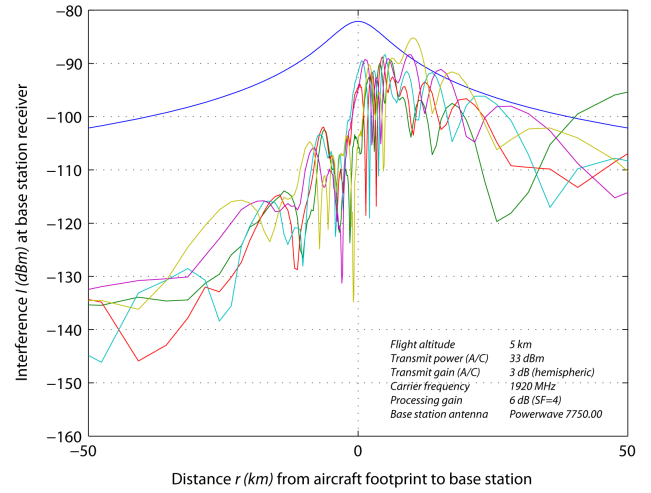
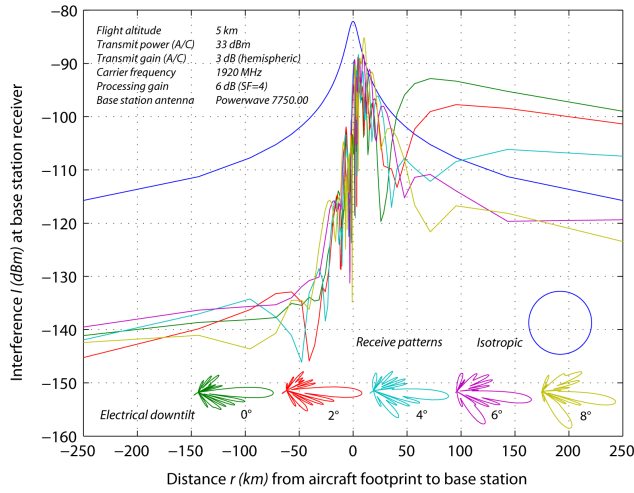


Figure 4.4: Interference at base station receiver as aircraft flies by for three typical antennas (the graphs on the right are closeups)

4 *Air-to-ground link model*

5 Description of uplink WCDMA physical layer simulator

As a second task of this thesis, a physical layer simulator for uplink UTRA FDD has been implemented in JAVA. The simulator is designed for the four uplink reference measurement channels, as specified by the 3GPP that can be used for different UMTS Quality of Service (QoS). As shown in Figure 5.1, the simulator consists of an initialization phase and an execution phase. During the initialization phase, we input all the values required to start the simulation which are read from a parameter file and these values can be changed accordingly for each simulation run based on the reference measurement channel.

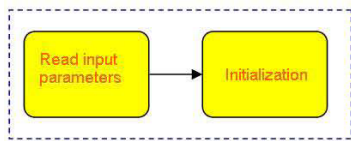
The execution phase consists of a loop that runs over the number of radio frames, which is passed as a parameter and whose value can be varied, for achieving the desired performance requirement of different UMTS Quality of Service. This is the main loop, during the execution of which we perform the operations that are done in the physical layer of the UE (User Equipment or transmitter). The data is then transmitted through different types of radio channels. The interference from the aircraft is considered at the receiver (Node B) of the terrestrial user. This is then followed by a sub method in the main loop that describe the processing that takes place in the Node B (base station), this sub method ends up in evaluating the errors (both bit and block) in the data received at the Node B (receiver) as compared to the original transmitted data.

Generally in UTRA the data generated at higher layers is carried over the air with transport channels. Transport channels are mapped in the physical layer to different physical channels. Two types of transport channels exist, dedicated transport (dedicated) channel and common channel. Here we consider only the dedicated transport channels for our implementation because the dedicated transport channels carry all the information intended for the given user coming from layers above the physical layer, including the data for the actual service as well as higher layer control information which are mapped to dedicated control channel (DCCH), carrying the user control data and dedicated transport channel (DTCH), carrying the user information data. The data generated in the DTCH is important as the execution phase ends up in performing the bit and block error rate evaluations of the user information data.

The data generation in the transport channels is executed by another sub loop inside the main frame loop that runs twice for the user control and information data. During the execution of each run a new set of data for the specific transport channel is generated based on the condition that whether it is the periodicity at which a transport block (TB) is transferred by the physical layer on the radio interface and this is always a multiple of the minimum interleaving period of

5 Description of uplink WCDMA physical layer simulator

Initialization Phase



Execution Phase

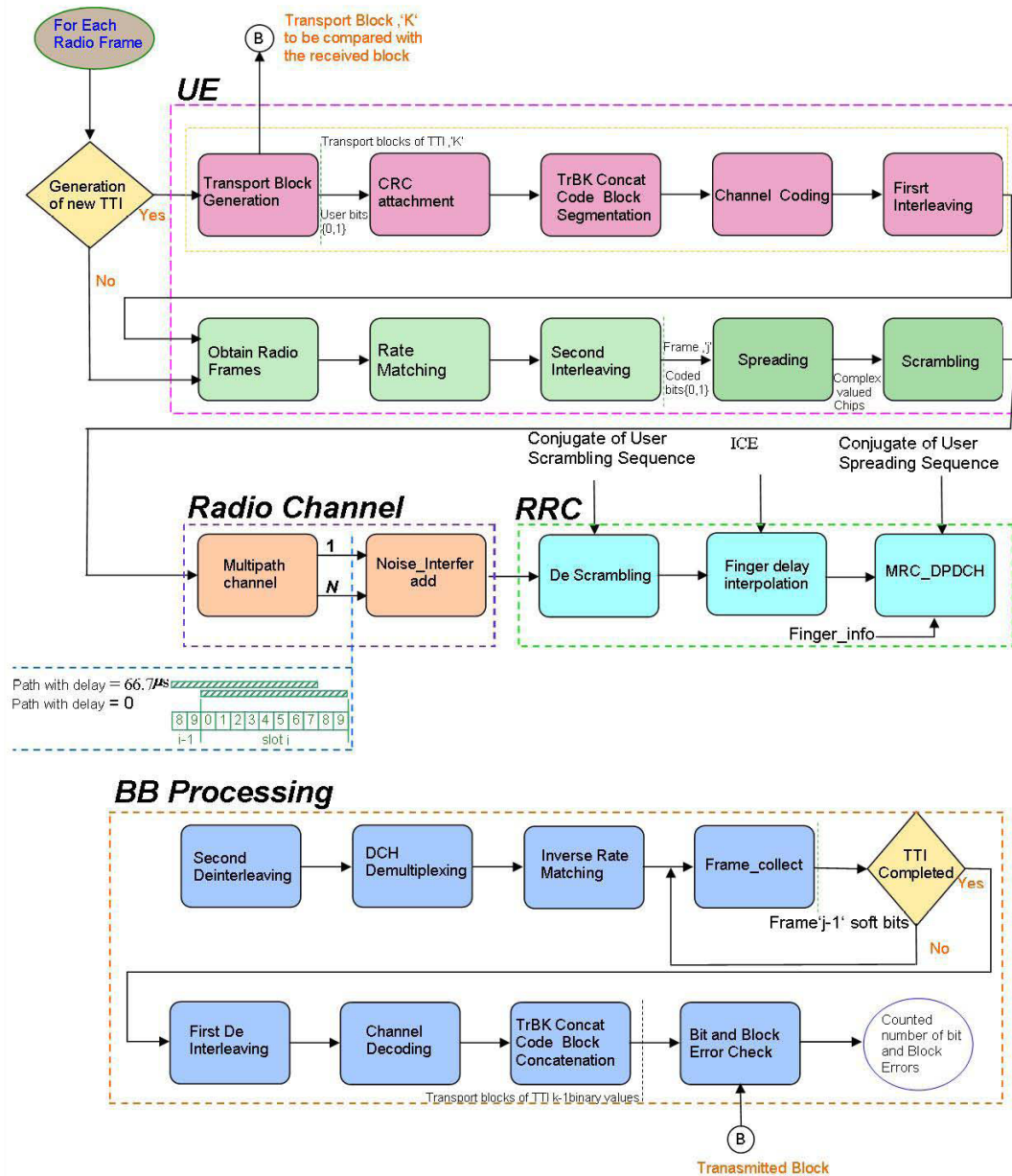


Figure 5.1: Description of the Simulator

one radio frame (10ms).

After the generation of new set of data on each transport channel the data of each transport channel (TrCH) must be processed.

Adding Cyclic Redundancy Check (CRC) bits to each transport block. The CRC bits help in the error detection of the transport blocks. The size of the CRC could be 24, 16, 12, 8 or 0 bits and it is generally signalled from higher layers, which is passed as a parameter for each transport channel (TrCH).

After adding the CRC bits, concatenation of all the transport blocks in a transmission time interval (TTI) is performed. Code block segmentation operation is done if the number of bits in a TTI is larger than the size of a code block. The code block size varies depending on the type of channel coding used for the transport channel. The code block size is '804' if convolutional coding is used and it is '5114' if turbo coding is used.

Code blocks are then delivered to the channel coding block. The following channel coding schemes have been applied to the data of the transport channels:

- Convolutional coding
Convolutional coding with constraint length 9 and coding rate $\frac{1}{3}$ is applied. For this type of coding scheme '8' tail bits, equal to the length of the shift register used in the convolutional encoder having a binary value '0' must be added to the code blocks before the encoding, to ensure that the encoding process ends up in a zero or initial state. The generator polynomials which describe the connection among shift registers and modulo 2 adders used for the Convolutional coding are 557(octal), 663(octal), 711(octal).
- Turbo coding
The scheme of turbo coder is a 'Parallel Concatenated Convolutional Code'(PCCC) with two 8-state constituent encoders and one turbo code interleaver. The coding rate of turbo coder is $\frac{1}{3}$. After the encoding operation, the encoders are forced back to the zero state and this process is called trellis termination. The trellis termination is performed by padding 12 bits of value '0' after the encoding of the information bits.

The size of the encoded block, 'Yi' is dependent on the coding scheme

- convolutional coding with rate 1/2 $Y_i=2*(\text{size of code block})+16$
- convolutional coding with rate 1/3 $Y_i=3*(\text{size of code block})+24$
- turbo coding with rate 1/3 $Y_i=3*(\text{size of code block})+12$

The choice of the channel coder can be done during the initialization phase depending on the type of the coding used for the transport channel. After the channel encoding of each block of user information and control data, a 'first interleaving' operation is performed for reducing the burst

5 Description of uplink WCDMA physical layer simulator

errors introduced by the channel and the interleaver that has been used for our implementation is a block interleaver with inter column permutations, as specified by the 3GPP. The sub loop ends up in generating the users information and control data. This data requires a further processing in the physical layer before being transmitted over the channel.

When the transmission time interval of the transport Channel is longer than 10 ms, the input bit sequence is segmented and mapped onto consecutive radio frames. Every 10 ms, one radio frame from each transport channel is multiplexed serially, first the user information data followed by the user control data. Rate matching operation is performed on the multiplexed data. In this implementation we perform the rate matching operation, when the rate matching pattern is used to puncture the input data and we add a binary value of zero, when we need to repeat some data values of the user frame in order to conform to the specifications. The result of the rate matching operation is to obtain a coded composite transport channel (CCTrCH). The so formed composite transport channels are interleaved by a 'second interleaver' which is a block interleaver that performs inter column permutations.

Now a mapping of the transport channels to the physical channels is carried in order to be transmitted over the air. A physical channel, in general is defined by its carrier frequency, channelization code (CDMA) and relative phase for the uplink connection. This phase is either 0 or $\frac{\pi}{2}$ corresponding to the in phase or quadrature component. In this implementation we consider the following Physical Channels

DPDCH–Dedicated Physical Data Channel:-

this carries the user control and information data. There may be zero, one or many DPDCH on each connection.

DPCCH–Dedicated Physical Control Channel:-

this carries control information related to the physical layer. There is only one DPCCH on each connection.

Transmission Characteristics:

The following transmission characteristics are used for all the Physical channels

- Modulationchip rate:3.84 Mcps
- Modulation:QPSK data and spreading modulation

The physical channels must be transformed to the transmission characteristics by applying the spreading operation which is described in the following section.

5.1 Overview of Spreading and Modulation

The spreading consists of two operations.

5.1 Overview of Spreading and Modulation

The first is the channelization operation, which transforms every data symbol into a number of chips, thus increasing the bandwidth of the signal. The number of chips per data symbol is called the ‘spreading factor’ (SF).

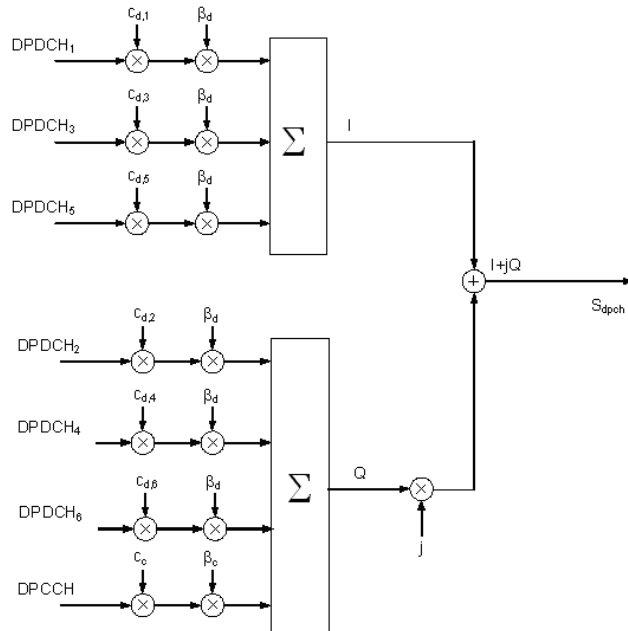


Figure 5.2: Overview of Spreading

The binary input sequences of all physical channels are converted to real valued sequences, i.e, the binary value “0” is mapped to the real value +1, the binary value “1” is mapped to the real value -1 . As shown in Figure 5.2, the spreading operation includes a spreading stage where the ‘DPDCH’ and ‘DPCCH’ are spread to the chip rate by the channelization code (c_d). With this operation the data symbols are independently multiplied with an ‘Orthogonal Variable Spreading Factor’(OVSF) code. The OVSF codes are used to separate the different channels that may be present on a certain frequency in a CDMA system, they also support a variety of data rates and Spreading factors, no matter what length they are. After the channelization operation the real valued spread signals are weighted by gain factors ‘ β_c ’ for DPCCH and ‘ β_d ’ for DPDCH. These weighting factors are signalled by higher layers (we input them as parameters whose values are initialized during the initialization phase). In this implementation we multiply the DPCCH chips with an amplitude ratio factor in order to assure that the power values of the DPCCH chip signals are less than those of the DPDCH, by doing, so we can assign more power for the DPDCH chip signals. This enable us to have a better detection of the user information data at the receiver (Node B). After performing the amplitude scaling operation, the real valued spread signals are mapped, DPDCH onto the I branch and DPCCH onto the Q branch and are summed up. Where I and Q denote the real and imaginary parts respectively. This results in a complex valued stream of chips for each set of channels.

5 Description of uplink WCDMA physical layer simulator

The second operation is the scrambling operation, which is the key operation of the UTRA FDD. With the scrambling operation, all users can transmit on the same frequency and are differentiated by using a unique scrambling code (complex valued sequence). The receiver has the scrambling sequence of the user, descrambles the received signal to recover the original data. The user data may be scrambled by either a long or a short scrambling code. In this implementation we have used long scrambling codes which are essentially ‘Gold codes’. It is known from theory that largest sets of Gold codes have low cross correlational properties, so that as many users can use the channel with minimum mutual interference, which allows a less complicated base station design at the receiver without using an advanced receiver or interference canceler. There are (16777216) long scrambling codes. The long scrambling sequences are constructed from position wise modulo 2 sum of 38400 chip segments of two binary m-sequences, generated by means of two generator polynomials of degree 25. The generated scrambling sequence is a pseudo random noise sequence (Gold sequence) improving the spectral properties of the signal.

In this implementation, we generate a new pair of scrambling sequences both for the user and the interferer after every 100 runs of simulation (radio frames) because it might happen that one particular pair of generated scrambling sequences might have good auto and cross correlation properties as compared to the other. By doing so we average the orthogonal properties of the scrambling codes which aids in producing precise results.

After spreading, the user data must be transmitted through the radio channel. Although the channel is quite often out of the designer’s scope, a realistic channel model is an essential prerequisite for the design of any communication system. In the study of signals and systems, the channel is viewed in terms of its input, its output and some description of how the input affects the output. If a channel was just a filter (Linear-time invariant system), then it could be completely characterized by its impulse response or frequency response. However, channels in practice have an extra ingredient: noise. For our implementation we use two types of channels that are mentioned in the following section.

5.2 Channel

AWGN channel : Additive White Gaussian Noise Channel is mainly used to estimate the channel coders.

The variance of the noise generated by the AWGN channel is calculated from

- $\frac{E_b}{N_o}$ is the ratio of bit energy to noise power spectral density in (dB)
- E_c is the power of the input chip
- L_c is the number of chips in the transmitted signal

- L_{inf} is the size of the user data per TTI

$$\frac{E_b}{N_o} = \left[\frac{E_c}{N_o} \right] \left[\frac{L_{chip}}{L_{inf}} \right] \quad (5.1)$$

According to formula (5.1) 'N0' is the total one sided noise power spectral density of all noise sources.

Multipath Channel : This is the more realistic channel found in today's mobile communication systems where the transmitted signal arrives at the receiver via multiple propagation paths at different delays. There are two important characteristics of the multipath channel, one characteristic is the time spread introduced in the signal that is transmitted through the multipath channel i.e. if we transmit an extremely short pulse, ideally an impulse, over a time varying mutipath channel, the received signal might appear as a train of pulses occurring after different delays. The second characteristic is due to the time variations in the structure of the medium. As a result of such variations, the nature of multipath varies with time. A 'tapped delay line model' was used for the multipath channel which can be configured by passing parameters from outside of the block. Four cases were used that are specified according to the 3GPP specifications and multipath channel block also adds noise, the variance of the noise is calculated according to formula (5.1).

Now the desired user signal is corrupted by the channel noise. This arrives at the base station (Node B). Here we have to consider the interference from the aircraft. The interference addition is performed directly by adding to the user data, the data from the aircraft at the receiver (Node B). The interferer signal is normalized with this SIR value which can be passed as a parameter from outside and whose value can be varied depending on the number of aircraft.

The degraded user data (both the information and the control data) is now at the base station which must be processed to extract the user information data.

At the receiver (base station or Node B) the sequence of operations done are inverse to those that are performed at the transmitter (User Equipment). First the received signal is descrambled by using the complex conjugate of the same scrambling sequence that is used for the user at the transmitter. Following the descrambling operation, the RAKE reception and maximum ratio combining is carried if multipath channel is used for simulation. Otherwise, the descrambled data is multiplied by the complex conjugate of the same spreading array that is used to spread the user data at the transmitter, to obtain an estimate of the user frame. The estimated user frame is deinterleaved by using the same intercolumn permutations that is used at the transmitter. Next the estimated frames are concatenated to obtain an estimate of the user transport blocks that were actually delivered to the physical channel. After the concatenation of the user estimated frames the first de interleaving operation is performed which is exactly the inverse of the interleaving operation performed at the transmitter by using the same intercolumn permutations.

5 Description of uplink WCDMA physical layer simulator

Until now all the estimates of the user information data are in soft values and not in bits, next we do the channel decoding operation and we use soft decision decoding which yields a better performance than the hard decision decoding.

The output of the channel decoding are a sequence of estimates of the user data bit stream which must be sent into the bit error and block error rate evaluation blocks which yields the number of bits and blocks that were different from original information data and these calculations are done excluding the Cyclic redundancy check bits.

6 Simulation Results

In this chapter, we present the results of the link level simulations, conducted to evaluate the performance degradation at the receiver (base station) for different interference levels. We use these results together with the theoretical formulae developed using the model 4.1 in chapter 4 to provide a quantitative analysis that illustrates the size of the airspace cell to the transmit power increase of the terrestrial user. First, the graphs showing the bit error rate (BER) and block error rate (BLER) are presented, from them we have chosen to use the block error rate (BLER) as a performance metric following 3GPP specifications since “**transport block**” is the unit of exchange of information between the MAC sublayer and the physical layer.

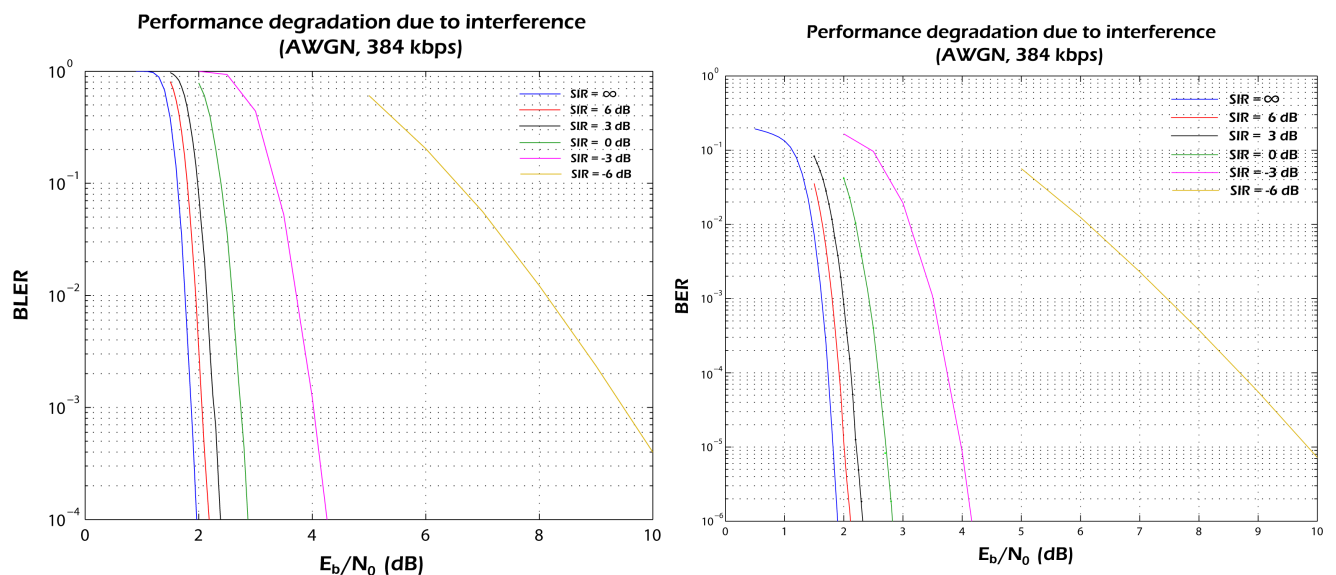


Figure 6.1: Bit and block error rate curves for user data rate of 384 Kbps, AWGN channel

From Figure 6.1, plotted according to the parameters listed in Table 6.1, we can observe that in order to achieve the same performance in bit or block error rate in the presence of interference, we need to increase the bit energy which is nothing but increasing the transmit power and this becomes even worse with higher interference i.e. to achieve a performance of 10^{-3} in block error rate, in the presence of a three interferers (shown by the magenta line), we need to increase the transmit power by 2.5 dB (approximately) as compared to the case when no interferer (shown by the blue line) is present. This is not always the same with bit error rate reminding that a block in error does not mean that all the bits in the block are in error. Now we consider the results of the simulation conducted according to the parameters listed in Table

6 Simulation Results

Reference measurement channel	384 Kbps
Number of radio frames	1,00,000
Channel coding for DTCH transport blocks per TTI	Turbo coding
Channel coding for DCCH transport blocks per TTI	Convolutional coding
DCCH amplitude scaling factor	0.333
Spreading factor	4
$\frac{E_b}{N_o}$ start	0dB
$\frac{E_b}{N_o}$ stop	10dB
Channel	AWGN

Table 6.1: Parameters for user data rate of 384 Kbps, AWGN channel

Reference measurement channel	12.2 Kbps
Number of radio frames	1,00,000
Channel coding for DTCH transport blocks per TTI	Convolutional coding
Channel coding for DCCH transport blocks per TTI	Convolutional coding
DCCH amplitude scaling factor	0.733
Spreading factor	64
$\frac{E_b}{N_o}$ start	5dB
$\frac{E_b}{N_o}$ stop	20dB
Channel	AWGN

Table 6.2: Parameters for user data rate of 12.2 Kbps, AWGN channel

6.2.

Figure 6.2, plotted for a user data rate of 12.2 Kbps, shows that to have a same performance in block error rate of 10^{-3} in the presence of three interferers (shown by the magenta line), we need to increase the transmit power by $< 1dB$ for the same AWGN channel. This clearly shows that the data rate of the desired user has a significant effect on the performance degradation irrespective of the data rate of the interferer. Processing gain $10\log_{10}^{Spreading\ factor}$, plays a role in improving the performance at the receiver.

Figure 6.3 shows the performance degradation by considering the realistic scenario, that the desired user now has a multipath channel and not the static AWGN channel. This figure is plotted for the parameters shown in table 6.3. By comparing figures 6.1 and 6.3 (if we look at the blue lines in the two figures, which are plotted for the case that no interferer is present, we can observe that in order to have a block error rate of 10^{-3} we need to give a bit energy of 2 dB if the channel is AWGN, which is 6 dB for multipath channel), it can be concluded that we have a better performance at the receiver when the user channel is AWGN, which is non realistic but even with multipath propagation channel, we can achieve a performance that matches closely

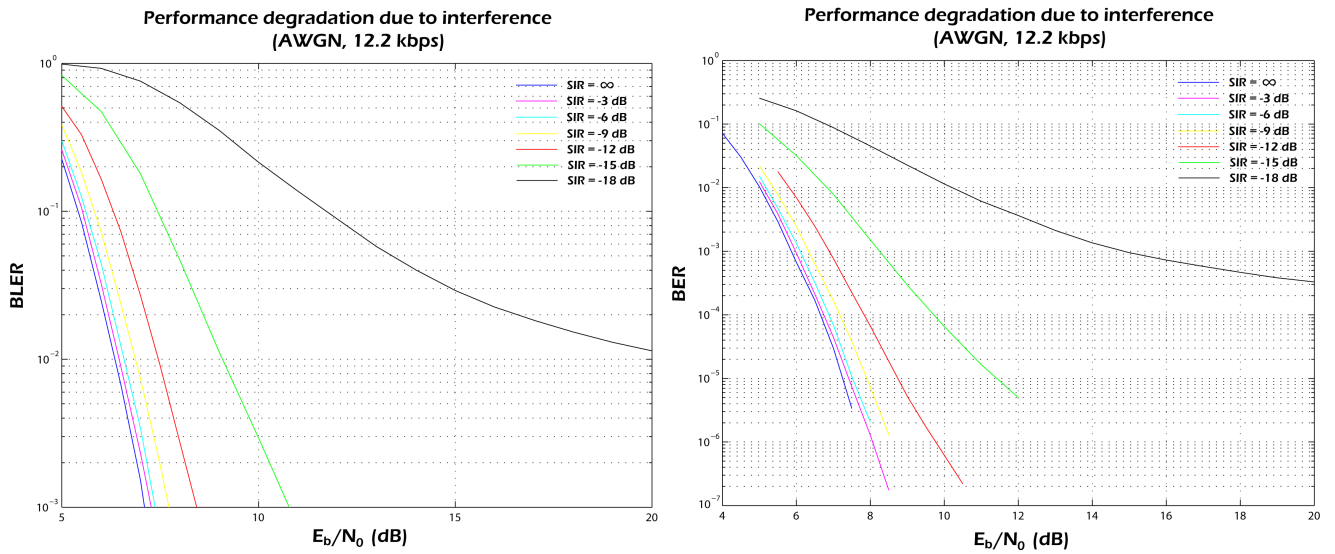


Figure 6.2: Bit and block error rate curves for user data rate of 12.2 Kbps, AWGN channel

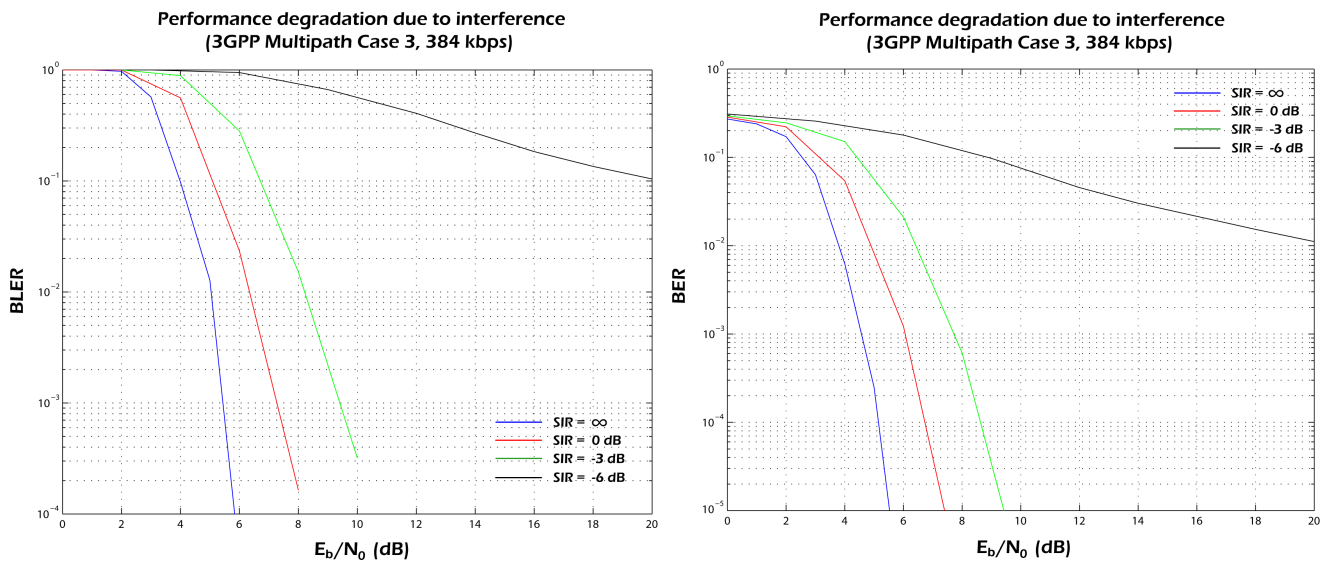


Figure 6.3: Bit and block error rate curves for user data rate of 384 Kbps, MP channel, TPC OFF

with the performance obtained when the channel is AWGN, by providing more replicas (fingers) of the transmitted signal. The RAKE receiver circuit takes advantage of these replicas (diversity) and performs the maximum ratio combining of all fingers at the receiver which improves the performance to a significant extent.

Now we present the figures that show a considerable improvement in the performance even with the multipath channel by implementing the "transmission power control" concept of the WCDMA. A detailed explanation about the transmit power control can be found in 2.2. In order

6 Simulation Results

Reference measurement channel	384 Kbps
Number of radio frames	1,00,000
Channel coding for DTCH transport blocks per TTI	Convolutional coding
Channel coding for DCCH transport blocks per TTI	Convolutional coding
DCCH amplitude scaling factor	0.733
Spreading factor	4
$\frac{E_b}{N_o}$ start	5dB
$\frac{E_b}{N_o}$ stop	20dB
Channel	Multipath
Doppler Spread	222.2222
Number of additional paths	3
TPC	off

Table 6.3: Parameters for user data rate of 384 Kbps, MP channel, TPC off

to apply the transmit power control concept we need to switch from simulating radio frames to slots i.e. we now divide the radio frame into slots and then transmit the slots over the channel and at the receiver, we combine all these slots to get back the radio frame. By doing so, we can consider that the channel response is not varying rapidly for a slot period and this helps us in evaluating channel estimates correctly. Figure 6.4 inputs the parameters listed in table 6.4 and from this it can be seen that in order to have a block error rate of 10^{-3} we need to give a bit energy of 2.5 dB (blue line) as opposed to the case when no “transmission power control” concept is implemented where we have to have a transmit power of 5.5 dB (approximately) to achieve the same performance (blue line) in Figure 6.3.

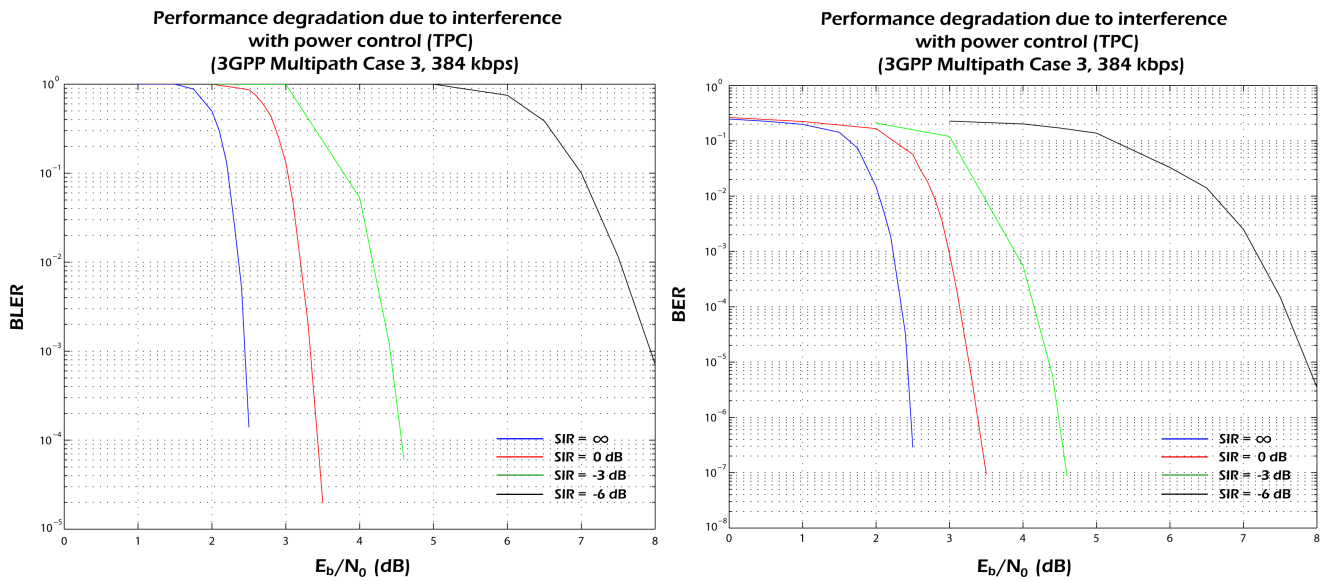


Figure 6.4: Bit and block error curves rate for user data rate of 384 Kbps, MP channel, TPC ON

6.1 Required UE power increase versus aircraft cell radius

Reference measurement channel	384 Kbps
Number of radio frames	1,00,000
Channel coding for DTCH transport blocks per TTI	Convolutional coding
Channel coding for DCCH transport blocks per TTI	Convolutional coding
DCCH amplitude scaling factor	0.733
Spreading factor	4
$\frac{E_b}{N_o}$ start	0dB
$\frac{E_b}{N_o}$ stop	8dB
Channel	Multipath
Doppler Spread	222.2222
Number of additional paths	3
TPC	on

Table 6.4: Parameters for user data rate of 384 Kbps, MP channel, TPC on

6.1 Required UE power increase versus aircraft cell radius

In this section, we intend to show the relationship between the maximum allowable airspace cell radius (within which the aircraft link exhibits the desired performance) and the cost in terms of transmit power increase required at the mobile terminal in order to maintain the performance of the terrestrial link in presence of interference from the aircraft at the base station receiver. In order to do so, we will use the raw data obtained from the simulation results to find the increase in transmit power for a satisfactory performance in the presence of different interference levels. We consider the case that the terrestrial user is transmitting at a constant data rate of 384 Kbps and we vary the transmission data rate of the aircraft (12.2 Kbps and 384 Kbps). We use the formula 4.11, to find the airspace cell radius, for an aircraft flying at an altitude of 10 Km and we find the value of α by assuming hemispheric transmitting antennas ($3dB_i$). Figure 6.5 illustrates the aircraft cell radius normalized to the flight altitude to the cost in terms of power of the terrestrial user for a typical base station receive patterns obtained from power wave 13. This figure is plotted for a base station receiver having a down tilt of 0° . The effect of changing the down tilt of the base station receiver antenna from 0° to 16° is shown in Figure 6.6. Figure 6.7 illustrates the airspace cell radius for different scenarios, the blue line is for the user link using a AWGN, the red line is for the user link using a multipath transmission channel and the green line is for the user link with multipath using transport power control phenomenon.

From figures 6.5, 6.6 and 6.7, we can observe that for a cell radius of 50 km, even at an altitude of 10 km and with a rather optimistic UEBS antenna pattern, the required power increase at the mobile terminal is around 3 dB. This clearly indicates that the ground infrastructure is very sensitive to radiation from aircraft in the same frequency band. Neither the skyward receive properties of terrestrial base stations nor the quasi-orthogonality of scrambling sequences are capable of making the interference negligible. We therefore conclude that an exclusive frequency band is

6 Simulation Results

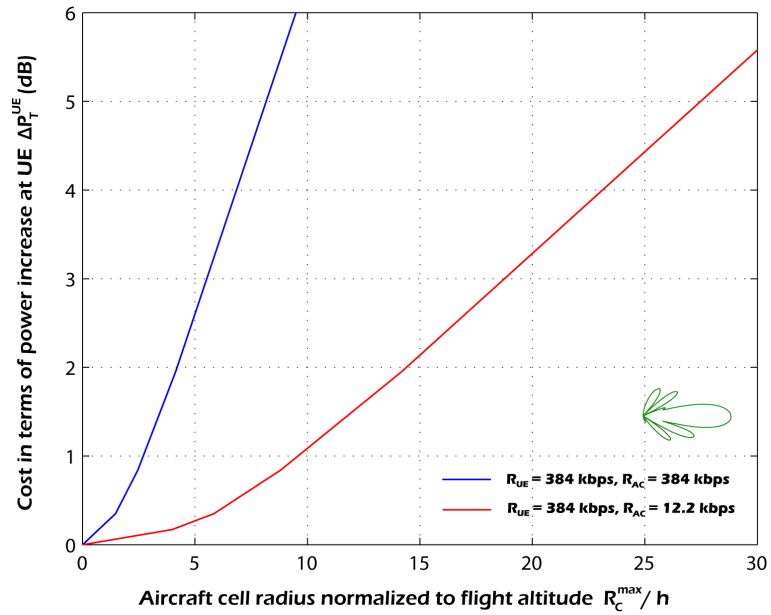


Figure 6.5: Dependency of the airspace cell size with the cost in terms of mobile terminal power increase for AWGN channel with 0° antenna down tilt

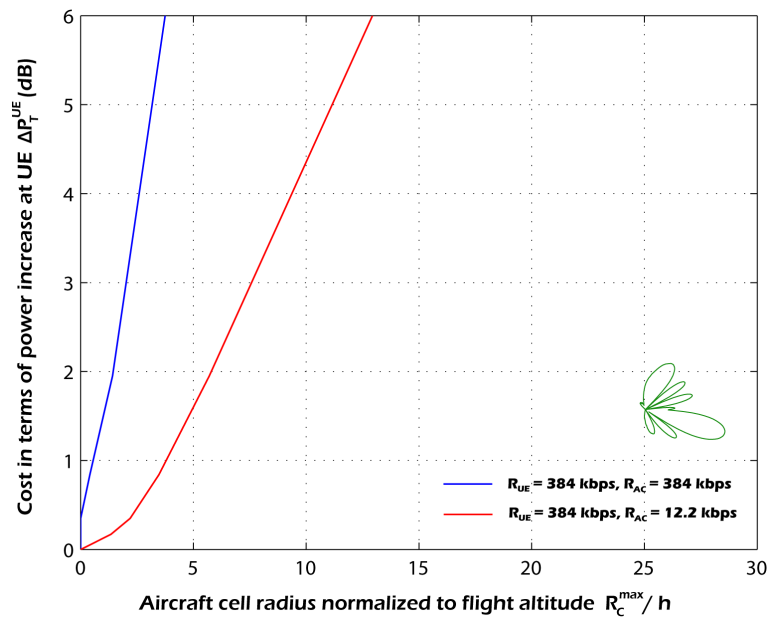


Figure 6.6: Dependency of the airspace cell size with the cost in terms of mobile terminal power increase for AWGN channel with 16° antenna down tilt

required, if both systems are to coexist.

6.1 Required UE power increase versus aircraft cell radius

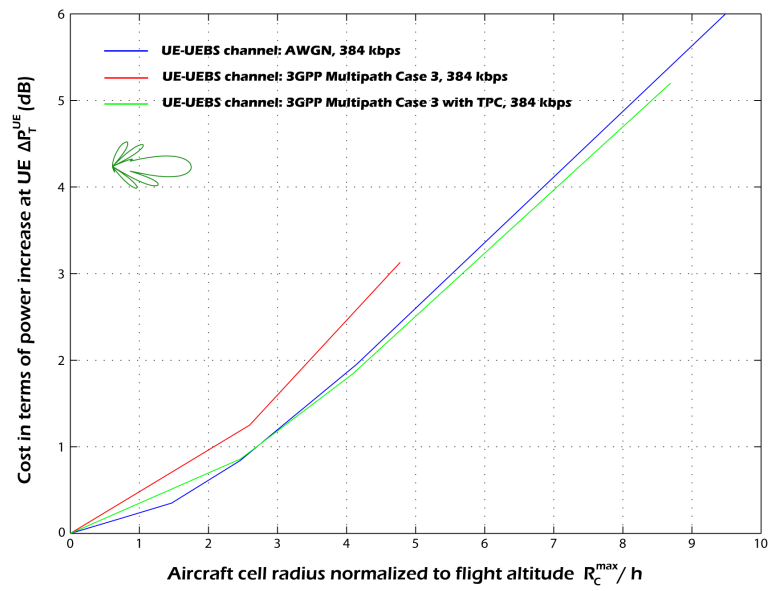


Figure 6.7: Dependency of the airspace cell size with the cost in terms of mobile terminal power increase for AWGN and MP channel (TPC) with 0° antenna downtilt

6 *Simulation Results*

7 Conclusions and Outlook

In this thesis, we have investigated the possibility of using UMTS for direct air-to-ground communications. This thesis has focused on the WCDMA air interface between Node B and UE at the physical layer, assuming that an aircraft takes the role of a UE.

In chapter (2), we mention the main design aspects of WCDMA that support a variety of functions like high variable user data rates, the basic modes of operation (FDD, TDD), the operation asynchronous base stations etc. The principle of power control has been discussed. The power control concept is critical, since it is the main form of resource allocation which is particularly important on the uplink where we have the many to one scenario. Without power control a single over powered mobile will block the whole cell. We also describe about different kinds of handover principles (soft, softer and inter RNC) that the UE can perform to maintain an ongoing call. We present the UMTS system architecture with a short introduction to all the network elements of the architecture and the different interfaces between these elements.

In chapter (3), we consider the idea of reproducing the cellular structure of the terrestrial UMTS in the airspace. Some aircraft specific constraints, such as Doppler shift, propagation delay, handover and interference have been identified and analyzed. Doppler shift occurs in terrestrial networks on a much smaller scale, since mobile stations on the ground move at much lower speeds. However, WCDMA receivers are equipped with powerful frequency acquisition circuits, capable of counteracting this effect. We have also shown that propagation delay has no significant effect on the power control mechanism. Finally, we have seen how UMTS networks can perform handover procedures between remote parts of the network, thanks to the I_{ur} interface.

Chapter (4) presents a prototype that illustrates the direct air-to-ground communication link. Based on this model, we derive the equations relating the airspace cell radius and the cost in terms of transmitter power increase at the terrestrial UE in the presence of interference from the aircraft. Later, we have concentrated on the receive patterns of the base station antennas, that provide us a first impression of the increase in the level of interference based on the position of the aircraft relative to the base station due to the skyward receive properties of the base station antennas. We mention the formula for evaluating the interference from the aircraft at the base station based on the link budget calculation and from this formula, we estimate the values for the worst case interference. Chapter(5) describes in detail about the simulator that has been used throughout this thesis work for conducting link level simulations.

During this thesis, we have focused much of our study on analyzing the possibility of using UMTS terrestrial frequencies for an aircraft component. It can be observed from the simulation

7 Conclusions and Outlook

results shown in chapter(6), that an aircraft component transmitting at these frequencies would degrade the performance of the existing network to an intolerable extent due to interference. This is mainly because the skyward characteristics of the mobile communication antennas deployed on the ground are such that any signal being transmitted at the UMTS reverse link frequencies from the sky would cause significant interference on the base stations.

The terrestrial network would react to this interference automatically by means of power control, commanding all users to increase their power. This produces the so-called “cell breathing” effect, which in this case makes the cell shrink, potentially leaving some users out of coverage, or reducing the data rate they can achieve. In order for the aircraft to degrade the performance of the terrestrial network only to a tolerable extent, it would need to transmit at extremely low power. The airspace cells would then have to be so small that the system would be impractical.

A lot of research work remains to be done. An important aspect in network planning is the distribution of users over the area where the network will be deployed. In this respect, an interesting input for a further study would be the aircraft distribution over the European airspace, particularly at rush hours, so that typical and maximum aircraft densities can be estimated. From this data, traffic demand and multiple access interference considerations would lead to an estimation of the appropriate cell size for the aircraft cellular system.

The results of this study should now be focussed on the survey of potential frequency bands, as well as an investigation of alternative technologies, in particular for the radio interface between aircraft and ground network.

A State of the art analysis

There are currently several companies in the United States intending to provide voice calls and Internet access on airplanes. They all agree that 2006 won't be the year that cell phones and other voice devices are widely usable on aircraft. They also agree that 2007 is a much more likely time-frame due.

The delay has less to do with developing technology than it does with regulatory and spectrum issues and satellite issues. And time also is needed to sort out the social issues related to providing voice service in the air. Many fliers have expressed deep concern about the noise and inconvenience of having a plane full of people talking on their phones at the same time.

However, the time is coming when voice calls and Internet access in the air will be common. First will come data access via Wi-Fi, a type of access that already can be found on a couple hundred long-haul planes today.

A.1 How voice will be added

Cell services will be added to existing aircraft by installing an on-board picocell, or a tiny cellular transmitter that would support GSM in Europe and both GSM and CDMA in the U.S. Depending on an airline's needs, the picocell could support just U.S. cell frequencies aboard domestic airliners or all frequencies used worldwide for cellular transmissions.

The picocell converts cellular packets into pure data for air-to-ground or air-to-satellite transmission. A ground station then pops the calls back into the phone system for completion. By the time the on-board equipment is installed, it's likely that older 2.5G and newer 3G services like GPRS, EV-DO, UMTS or HSDPA will be available.

Equipment manufacturers, airlines, and in-air telecom firms have completed tests in the U.S. and abroad to demonstrate that the technology already exists to make these offerings work and that they are safe to operate on planes.

A.2 Regulations

Three roadblocks remain to rolling out these in-the-air voice and data services for which the technology already exists. The first is an auction by the Federal Communications Commission (FCC) of a small swath of spectrum in the 800 MHz range, which the FCC is repurposing for direct air-to-ground communications. The auction will take place on May 10, 2006 and there could be one or two winners.

The second involves both the Federal Aviation Administration (FAA) and the FCC. The FAA wants continued testing to ensure that operation of cell phones on planes won't cause any unintentional interference with on-board avionics, as well as ensuring that, for security reasons, the service has the right controls. A pilot, for example, should be able to sever the voice link for passengers.

The FCC's interest lies in licenses that cellular carriers own for frequencies on the ground that winning bidders for the air-to-ground spectrum would like to use on an aircraft so that existing cellular devices would work. (Similar issues in other countries may be resolved sooner).

The other broad area of concern can best be classified as social issues. Many, including some in the airline industry, have expressed concern about how annoying it could be to be in a plane full of people having cell phone conversations.

A.3 Some Players

Of the several companies likely to make hay from the U.S. bidding, only Connexion by Boeing has a currently-operating data service on commercial flights, and only on long-haul flights by non-U.S. carriers. The other important firms are OnAir, AirCell and Verizon AirFone, each of which currently operates in a unique niche in the aeronautical telecom or data worlds.

A.3.1 Connexion by Boeing

Connexion uses a satellite downlink to provide access. Its service is installed on an estimated 200 planes operated by seven airlines, including extensive long-haul routes run by Lufthansa. Two more airlines will be added soon, while more are committed for future deployment. Connexion has a slight incumbent benefit as a division of airplane maker Boeing.

The service offers 5 Mbps downstream and 1 Mbps upstream, although each user may be throttled to lower download speeds. Voice-over-IP is a popular use for the service, which can cost \$10 to \$35 per flight depending on payment plan and flight duration. While Connexion hasn't formally stated it will bid on the air-to-ground spectrum, they do plan to add voice service once regulatory issues are resolved. Connexion serves just nine airlines, all non-U.S., on 170 flights. Its

business plan focuses on long-haul flights by wide-body aircraft and doesn't include significant North American domestic traffic.

A.3.2 OnAir

Satellite-based rival OnAir is a joint venture formed early 2005 from the assets of Tenzing, an early Connexion competitor that was formed by ex-Boeing employees, along with Airbus and SITA, a European airline-owned systems integrator.

OnAir is in a holding pattern at the moment as its satellite partner Inmarsat launches fourth-generation broadband "birds" with beam-focusing abilities. The second of three satellites launched in early November, but shakedown will take some time. OnAir expects limited aeronautic broadband to be turned on by late 2006; this will allow them to offer GSM-based cellular voice service in Europe. It will offer data services via modules that will ultimately offer 432 Kbps each per plane, with longer-haul aircraft having two or four modules (864 Kbps or 1.7 Mbps).

OnAir is not expected to be part of the U.S. spectrum auctions but could partner with a winning bidder to allow overseas flights to hand off from expensive satellite to cheaper ground bandwidth.

A.3.3 AirCell

US-based AirCell has a long history of operating air-to-ground telecommunications stations across the country for private flights. The company has an advantage: as an equipment maker, they'll benefit from selling gear to a winning spectrum bidder even if their bid fails.

AirCell has installed special upturned antennas on an existing 125 cellular base stations across the US, with which it plans to backhaul data and voice over WiFi connections, passing them on into the PSTN network, without the need for a satellite. In late 2005 AirCell announced the successful completion of its extended airborne demonstration program that allowed potential airline customers and others to experience the AirCell Broadband System's technology in flight. Targeted for commercial deployment in 2007, the AirCell Broadband System will enable airline passengers to use their own Wi-Fi and cellular devices such as laptops, PDAs, phones and Blackberries in a fully integrated wireless cabin over an affordable, broadband air-to-ground link.

AirCell has accumulated hundreds of hours of hands-on flight test experience with airborne wireless broadband, and the demonstration program marked a number of important technological firsts achieved by the company: the first end-to-end demonstration of wireless broadband using a direct air-to-ground link; the first use of advanced wireless technology for a broadband air-to-ground link; the first support of CDMA, GSM, VoIP and Wi-Fi over a common air-to-ground pipe; the smallest broadband antenna ever used in aviation (weighs 5 ounces; 4" tall); the highest speeds, altitudes and distances ever reached for EVDO technology.

The infrastructure on the plane consists of a picocell and a hotspot environment for mobile and

A State of the art analysis

WiFi, forwarding data to a front-end converter which sends an IP signal over a 3 megabit pipe to the antennas on the ground.

The flight demonstration program showcased an advanced technology prototype of the AirCell Broadband System. Key demonstration system components and technical features included:

- A Broadband Air-to-Ground Link that uses custom-designed EVDO wireless technology. The link provides a high-speed connection directly from the aircraft to the ground, delivering a "to-the-seat" user experience similar to a DSL link on the ground.
- A Cabin Telecommunications Router (CTR) that provides a high-speed, in-cabin hotspot for Wi-Fi-equipped devices (802.11b/g) including Voice over Internet Protocol (VoIP) phones.
- Multiple Cabin Picocells supporting CDMA and GSM voice communications for commercial cell phones.

AirCell remains the only company ever to receive regulatory approval to use cellular frequencies for airborne telecommunications. Having operated its own terrestrial network in the United States for many years, AirCell has more patents and experience applying cellular technology in the airborne environment than any organization in the world.

Building on its success, the company is now leveraging this unique experience in developing its next generation of airborne connectivity – bringing affordable broadband voice and data services to airline passengers. Operating over a new, next-generation digital network in North America, the AirCell Broadband System is targeted for commercial deployment in 2007. Pending the acquisition of the spectrum license from the FCC, the AirCell network will initially cover the continental U.S. and will be expandable to include Canada, Mexico and the Caribbean. AirCell's system will be US- or, at best, North America-specific, whereas the satellite-based services can clearly extend across the globe. There is a possibility that OnAir could use the AirCell network for the North American portion of long-haul flights, then switch to satellite when necessary. This would lower its costs for that portion, enabling either more competitive pricing or fatter margins, depending on the competitive environment when it comes to market, which is also set for the second half of 2006.

A.3.4 Verizon AirFone

Verizon AirFone has the incumbent advantage – it still has seatback phones on many airliners and has had no airborne competitors for several years. Calls from seatbacks and armrests over the U.S. are almost entirely made over their existing network.

Verizon AirFone will retain a sliver of frequency for use with their older technology for calling regardless of the auction's outcome, but the company is eager to upgrade services. It is expected

that it would take about a year from the close of an FCC auction to have equipment manufactured, tested in the air, and up and running on a commercial basis. Verizon is well positioned to bid in the auction and could win the full bandwidth. It has a significant advantage on the many planes already equipped with their service. A new antenna would need to be added on the plane's belly.

Verizon expects at least 2.4 Mbps connections to the ground through a network of 130 to 150 base stations. Even with a number of planes in the air connecting to the same base stations, the user would experience very high speeds, comparable to DSL.

If Verizon wins control of the air-to-ground channel, it is expected that Boeing would cut a deal with the wireless company so that its Connexion customers could use the Verizon network aboard aircraft flying domestically and not equipped with the satellite system.

That would leave Boeing tiny profit margins for service on those domestic flights, but at least would provide full coverage so that Connexion wouldn't lose customers.

Verizon aims to begin service just a year after it wins the license. The company can use its cell towers as sites for the ground stations.

Verizon plans to partner with other wireless companies so that passengers can access the service through their own providers. It will be able to offer passengers rates comparable to hotel Internet rates, which he cited as \$11 to \$15 a day. Connexion charges \$27 for a day.

All major U.S. carriers have expressed interest in the Verizon system, including prospective Connexion customers who want to integrate the two systems - using Connexion for transoceanic flight and air-to-ground domestically. No one really knows how high the auction bids will go because the air-to-ground airwaves will service a niche market of uncertain size.

The FCC does not pin a value on the airwaves, but spectrum auctions typically fetch a price about five times the pre-set minimum opening bid. Based on that rule of thumb, the bidding for the key air-to-ground airwaves could go to around \$15 million. But that's only the beginning of the required investment. Whoever wins must then build ground infrastructure, court airline customers, install equipment on airplanes and market to passengers.

A.4 Auction News

The Federal Communications Commission's (FCC) auction of two nationwide Air-Ground spectrum licenses in the 800 MHz band ended on June 2, 2006, the auction began on May 10, 2006 and closed after 144 rounds of bidding. The winning bidders for the two licenses were AC BidCo LLC and LiveTV, LLC. Ac Bidco, which teamed up with AirCell Inc., has won the three megahertz of spectrum. That is enough capacity to offer in-flight Internet services. LiveTV

A State of the art analysis

has won the one megahertz spectrum will become a wholly subsidiary of JetBlue Airways which is Newyork's low-fare airline. This spectrum is enough for services such as communications with cockpit from the ground.

The four MHz of Air-Ground spectrum in the 800 MHz band can be used to provide a range of communications services to passengers on commercial and other aircraft, including broad-band internet access. The auction however does not affect the Federal Aviation Administration's (FAA's) and aircraft operator's rules and policies restricting the use of personal electronic devices (PEDs) on aircraft. In addition, the auction does not affect the FCC's ban on the use of wireless telephones on airplanes, which is intended to help prevent possible interference to terrestrial wireless systems.

B Performance of RAKE Receiver

Now, we present the simulation results, used to evaluate the functionality of the RAKE receiver circuit used in the simulator 5 and to compare it with the theoretical Rake receiver performance obtained from 21.

Let us consider the transmission of binary signals (S_1, S_2) that have equal energy and are antipodal ($S_1 = -S_2$). In order to derive the error rate performance of the RAKE receiver, we have assumed that the channel estimates are perfect. This is possible if the channel fading is sufficiently low, i.e. $\frac{\Delta t_c}{T} \geq 100$ where T is the signaling interval and Δt_c is the coherence time of the channel. Furthermore, we assume that the spreading codes generated from pseudo random sequences are perfectly orthogonal, which result in signals that have good cross and auto correlation properties. The formulae below B gives us a procedure to calculate the error probability using the RAKE receiver.

$$BER = \frac{1}{2} \sum_{k=1}^L X_k \left[1 - \sqrt{\frac{\gamma_k(1 - \rho_r)}{2 + \gamma_k(1 - \rho_r)}} \right] \quad (\text{B.1})$$

where 'L' defines the number of paths or fingers, ρ_r is '-1' for antipodal signals

X_k is defined as

$$X_k = \prod_{\substack{i = 1 \\ i \neq k}}^L \frac{\gamma_k}{\gamma_k - \gamma_i} \quad (\text{B.2})$$

and γ_k is the average SNR for the kth path, defined as

$$\gamma_k = \frac{E_b}{N_o} (\text{linear}) E(\alpha_k)^2 \quad (\text{B.3})$$

Where $E(\alpha_k)^2$ is the mean square value of the channel impulse response of the kth path.

B Performance of RAKE Receiver

As shown in Figure B.1 where the solid lines (blue) shows the bit error rate performance evaluated using the theoretical formula (B for the rake receiver circuit for 2 paths), for the rayleigh fading channel and for the AWGN channel and the dotted line shows the same bit error rate performance, plotted using the RAKE receiver of the simulator that has been used throughout this thesis to evaluate the bit error rate performance. The simulations were conducted without the channel coding and interleaving operations.

As can be seen from the figure the two curves (the solid and the dotted) match closely with each other indicating that the RAKE receiver that was used in the evaluation of the bit error rate performance is in close agreement with the theoretical RAKE receiver circuit performance.

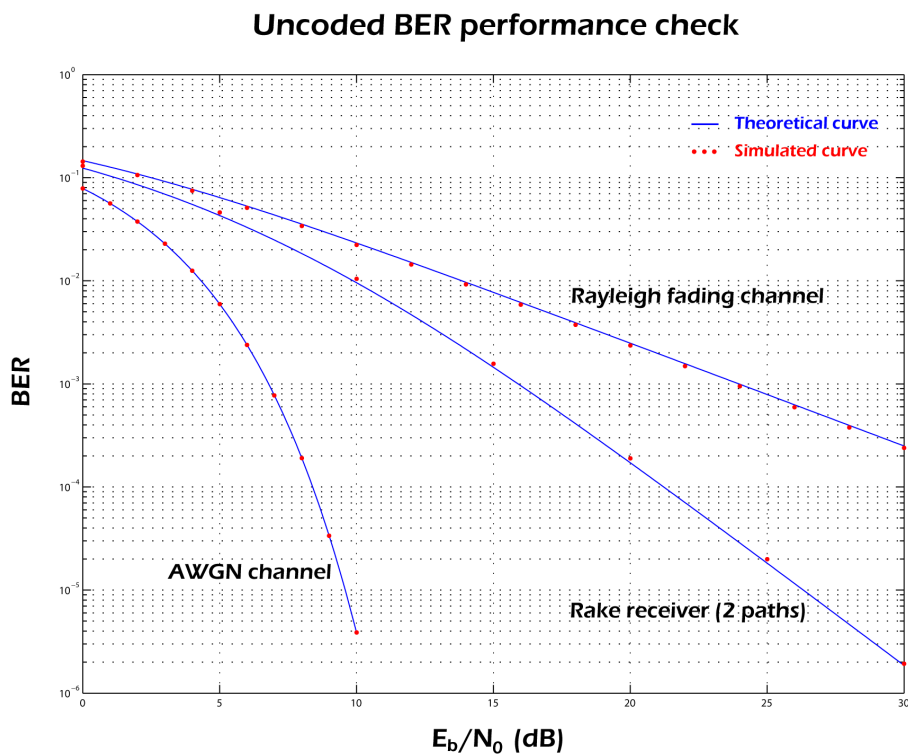


Figure B.1: Uncoded bit error rate check

C Mathematical derivations

Here, we present the equations used to determine the probability density function of the flight path length within the same cell. In order to derive these equations, we consider a circular airspace cell having a radius R_c . This is shown in Figure C.1.

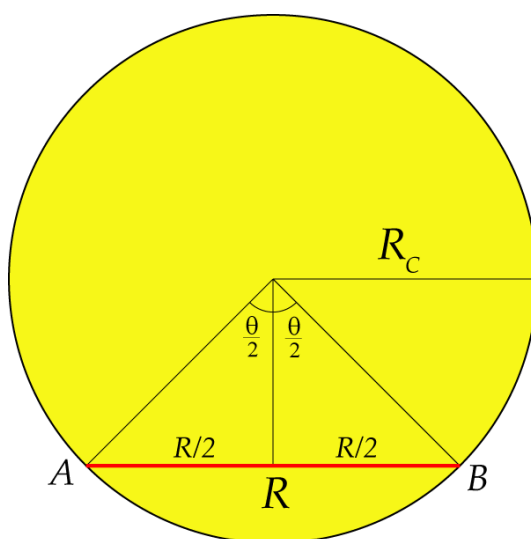


Figure C.1: Computation of $f_R(r)$

Aircraft trajectories are assumed to be linear. Points A and B indicate the locations at which the aircraft enters and leaves the cell, respectively. θ is the angle subtended by the intersections of the aircraft trajectory with the cell boundary. This angle is assumed to be uniformly distributed between 0 and π . The probability density function for θ is

$$f_{\theta}(\theta) = \frac{1}{\pi} \quad 0 \leq \theta \leq \pi \quad (\text{C.1})$$

The relationship between the length of the aircraft flight trajectory R and θ is

$$R = 2R_c \sin \frac{\theta}{2} \quad (\text{C.2})$$

C Mathematical derivations

The cumulative distribution function of the aircraft flight trajectory R is

$$F_R(r) = P[R \leq r] = P\left[2R_c \sin \frac{\theta}{2} \leq r\right] = P\left[\theta \leq 2 \arcsin \frac{r}{2R_c}\right] \quad (\text{C.3})$$

where $0 \leq r \leq 2R_c$.

Since the cumulative distribution function is the integral of the probability density function, we have

$$F_R(r) = \int_0^{2 \arcsin(\frac{r}{2R_c})} \frac{1}{\pi} dr = \frac{2}{\pi} \arcsin\left(\frac{r}{2R_c}\right) \quad (\text{C.4})$$

We obtain the probability density function of the aircraft flight trajectory as

$$f_R(r) = F'_R(r) = \frac{1}{\pi R_c \sqrt{1 - \left(\frac{r}{2R_c}\right)^2}} \quad 0 \leq r \leq 2R_c \quad (\text{C.5})$$

The probability that the aircraft is within the range $R_c \leq r \leq 2R_c$ is

$$P[R_c \leq r \leq 2R_c] = \int_{R_c}^{2R_c} \frac{1}{\pi R_c \sqrt{1 - \left(\frac{r}{2R_c}\right)^2}} dr = \frac{2}{3}. \quad (\text{C.6})$$

Bibliography

- [1] "Base station (BS) radio transmission and reception (FDD)", 3GPP Technical Specification 25.104 available at <http://www.3gpp.org/ftp/Specs/html-info/25101.htm>
- [2] "User Equipment (UE) radio transmission and reception (FDD)", 3GPP Technical Specification 25.101 available at <http://www.3gpp.org/ftp/Specs/html-info/25101.htm>
- [3] "Multiplexing and channel coding (FDD)", 3GPP Technical Specification 25.212 available at <http://www.3gpp.org/ftp/Specs/html-info/25212.htm>
- [4] "Spreading and modulation (FDD)", 3GPP Technical Specification 25.213 available at <http://www.3gpp.org/ftp/Specs/html-info/25213.htm>
- [5] "Physical channels and mapping of transport channels onto physical channels (FDD)", 3GPP Technical Specification 25.211 available at <http://www.3gpp.org/ftp/Specs/html-info/25211.htm>
- [6] "Physical layer - General description", 3GPP Technical Specification 25.201 available at <http://www.3gpp.org/ftp/Specs/html-info/25201.htm>
- [7] "Radio interface protocol architecture", 3GPP Technical Specification 25.301 available at <http://www.3gpp.org/ftp/Specs/html-info/25301.htm>
- [8] "UTRAN Iur interface general aspects and principles", 3GPP Technical Specification 25.420 available at <http://www.3gpp.org/ftp/Specs/html-info/25420.htm>
- [9] "AirCell readies direct air-to-ground WiFi for US flights", 26th April 2005, available at www.cbronline.com
- [10] "AirCell demonstrates in-flight wireless broadband using EVDO", 25th October 2005, available at www.evdoinfo.com
- [11] "Voice and data up in the air", Glenn Fleishman, 15th November 2005, available at www.mobilepipeline.com
- [12] "Rival emerges to Boeing's in-flight broadband", 23rd January 2006, available at <http://seattletimes.nwsources.com>
- [13] Radiation Pattern 3.0, Powerwave Technologies, available at <http://ww2.allgon.se/SYrp3/index.html>

Bibliography

- [14] "790-2500 MHz Base Station Antennas for Mobile Communications", Kathrein, available at www.kathrein.de
- [15] UMTS World antenna page: www.umtsworld.com/industry/antenna.htm
- [16] UMTSlink, www.umtslink.at
- [17] UMTS World, www.umtsworld.com
- [18] "WCDMA for UMTS: Radio Access for Third Generation Mobile Communications", edited by Harry Holma and Antti Toskala, Nokia (Finland), 2000 John Wiley and Sons, Ltd.
- [19] "UMTS and mobile computing", A. J. Huber and J. F. Huber, 2002 Artech House.
- [20] "UMTS networks: architecture, mobility and services", H. Kaaranen et al., 2001 John Wiley and Sons, Ltd.
- [21] "Digital communications", John G. Proakis, 3rd edition, McGRAW-HILL international editions